Överex finns

Light and Current Measurements from Prebreakdown Events in Laser-triggered Electrical Breakdown in Transformer Oil

LRAP-150

A diploma work performed by:

Jonas Bäckman

Abstract: The correlation between current and emitted light from prebreakdown events is good.Time lags in the laser triggered breakdown process have been analysed with help of simple models. The process seems to be best described as a five step process: trigger mechanism, bubble expansion, first connecting streamer, second connecting streamer and electrical breakdown.

Contents

1 INTRODUCTION

I have had the opportunity to perform my diploma work at the Department of Physics, Lund Institute of Technology. There my supervisor A.Sunesson, S.Kröll and P.Bårmann have built and designed an experimental set-up that has been used for their project "Laser spectroscopic investigations of dielectric breakdown". This has been part of a co-operative project with ABB Corporate Research. In their work they had to collect the emitted light from the prebreakdown events in order to resolve the spectral components. My work constituted of a similar part, where I was to resolve the emitted light in time. Therefore I could use a lot of their equipment which spared me a lot of time and work.

1.1 Scope of the diploma work

My task was to measure the correlation between emitted light and current during the prebreakdown events in laser triggered electrical breakdown. Since no complete measuring system for light that fulfilled the requirements for the mission was available, the first part of the work was to design and construct such a system. This is described in chapter two.

The second part consisted of measurements. Light and current were recorded, when different variables were altered, in order to check the correlation and to seek some characteristic features of the triggered breakdown process. The results are presented in chapter three.

The last part of the work was to analyse the collected data. Simple models have been used in order to explain the observed results. This is done in chapter four.

1.2 Electric breakdown

The study of electrical breakdown (EBD) in dielectrics has been a serious challenge to physicists and engineers for nearly one century [1]. In the case of gaseous dielectrics the phenomenon is fairly well understood. There it can be explained by avalanche ionisation.

When it comes to liquids such simple pictures do not exist. Many aspects of electrical breakdown in liquids have been investigated over the last decades but it has been hard to reconcile all the different results and conclusions that have been produced. Therefore, today, a general theory applicable to liquids does not exist.

The electric breakdown in dielectric liquids is a process of great economic importance. For instance, power transformers use dielectric liquids for insulation, and it is of great importance to be able to prevent breakdown from occurring.

In a configuration with two electrodes at different potential with an insulating dielectricum between them, an electric breakdown can occur as the result of different courses of events.

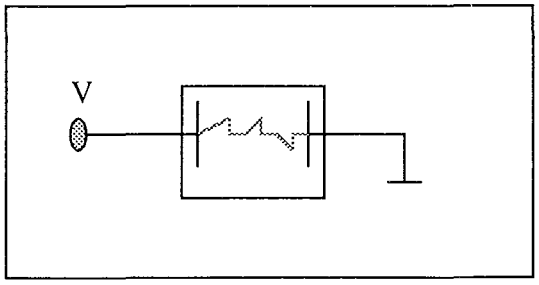

Fig [1.1] Breakdown

One simple way to produce electric breakdown is to slowly increase the potential at one of the electrodes. Thus, when the voltage is high enough, breakdown will occur. This is a so called spontaneous breakdown. Another way to produce electric breakdown, at a lower voltage than was needed for the spontaneous breakdown, is to trigger the system. There are many ways to trigger a breakdown, for instance the use of laser pulses,

sparks etc. In this work most of the experimental data comes from electric breakdown triggered by a Nd:YAG laser pulse, as will be shown later on in this report.

But what is an electric breakdown actually? Following a formal definition, it can be explained as a hot plasma-channel connecting two electrodes. The plasma is conducting and luminous, therefore breakdown is usually accompanied by large light and current pulses. The energy supply to this luminous arc is governed by the voltage source.

1.3 Prebreakdown process

The electric breakdown is the last event in a sequence of events that can be summarised into the prebreakdown process. In the literature concerning electric breakdown it is this phase that has mostly been investigated.

In order to describe the prebreakdown phase one has to take into account the many parameters that affect the process.

1.3.1 Electrode geometry

The shape of the electrodes will affect the electric field (E) in the dielectric liquid. Three types of electric fields are to be distinguished:

1 Inhomogeneous

2 Semihomogeneous

3 Homogeneous

In the literature one finds that the most frequently used geometry is the point-plane geometry [2, 3, 4, 5, 6, 7].

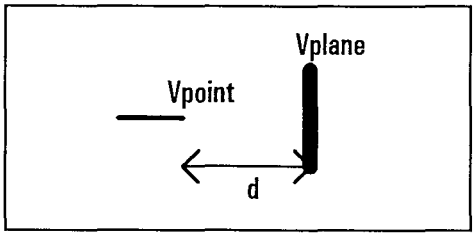

Fig [1.2] Point-plane gap.

It is a geometry that produces an inhomogeneous electric field with very high electric field strength at the tip of the point, see fig [1.2]. The tip radius has been observed to be an important parameter for the development of the process.

A homogeneous field can be produced by choosing two planes as electrodes, if one neglects the effect at the edges.

If the shape of the electrodes is hemispherical a semihomogeneous field will be the result when the voltage between anode and cathode is applied. This is true if the radius (R) is of the same size as the gap length (d), see fig [1.3]

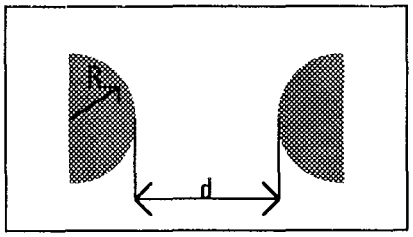

Fig [1.3] Hemispherical electrodes.

1.3.2 Applied voltage

There are three different types of voltage that can be applied to the electrodes:

1 Step voltage

2 AC voltage

3 DC voltage

The main difference between these three voltage fields is that in 1 and 2 there is a sudden change in voltage, which will act as a perturbation on the system and therefore enhance the probability of initiation of the process.

Step voltage and AC voltage is the far most used ([8, 9, 10]) but DC voltage has also been investigated ([6, 11, 12]).

1.3.3 Polarity

Since one electrode has a zero potential (at least in DC and step voltage) the other is associated with a certain polarity, +/- HV (high voltage). The polarity can be used to categorise the process into two classes:

1 Negative gaps

2 Positive gaps

With AC voltage it is standard to describe the gap as negative, when the streamer inception occurs at the electrode with a negative potential and vice versa.

1.3.4 Gap length

The distance between the electrodes is known as the gap length and can be subdivided into two classes:

1 Small gaps

2 Large gaps

There is no exact limit when the description of the gap length changes from small to large. In the literature one finds limits from five [13] to tens of millimeters. Most of the studies of prebreakdown events have been performed in small gaps but large gaps have been used as well ([14, 13])

1.3.5 Insulating medium

The properties of the dielectric liquid, such as density, viscosity and electronic properties, affect the prebreakdown process [2, 15]. In the literature concerning electric breakdown one finds that a lot of different liquids have been used (transformer oils, mineral oils, hydrocarbons etc.).

The prebreakdown process can thus be categorised using the parameters described above, but what is actually happening during this phase?

1.3.6 Streamers

In the early 1960's it was reported that electric breakdown was preceded by the development of a disturbance [16, 17]. This disturbance could be photographed using shadow-graphic technique [18] because it had altered refractive index. After this breakthrough in visualisation the technique has frequently been adopted. The disturbances described above are today called streamers and can be thought of as rapidly developing filamentary luminous channels [19].

The streamer is charged and is associated with a certain polarity. The polarity of the streamer is known when the direction of propagation is found.

- A positive streamer is starting from the anode (+) and propagates towards the cathode (-). Positive streamers propagate in the direction of the electric field (E).
- A negative streamer starts from the cathode (-) and propagates towards the anode (+). Negative streamers propagate in the opposite direction of the electric field (E).

There are two main classes of streamers, filamentary and bush-like. A filamentary streamer looks like a tree with the root at the starting point. The branches of the tree consists of fast developing thin channels. A bush-like streamer looks, as it sounds, like a bush, see fig [1.4].

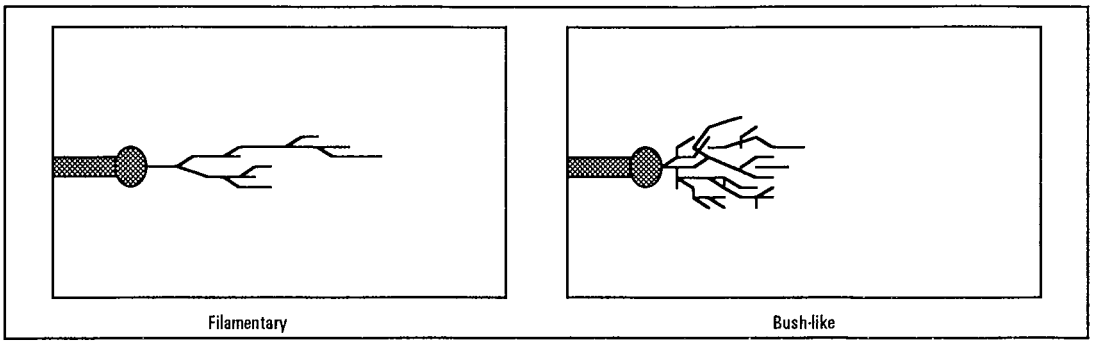

Fig [1.4] Two different types of streamers.

The bushlike streamer exists in both polarities and is slower than the filamentary one. The velocity is in the subsonic range (hundreds of m/s) [15]. The shape of the bushlike streamer is almost spherical. Energy studies of the growth of the bushlike streamer reveals that vaporisation of the liquid is the dominant process involved in the growth. Light and current pulses are always observed with bushlike streamers. These pulses are supposed to be due to discharges in the expanding gas phase [10]. The main energy injection for the growth process of the streamer comes from these discharges. When the electric pulses cease, the expansion is stopped.

Filamentary streamers are faster than bushlike. The velocity is in the supersonic range (km/s). The positive ones are usually one order of magnitude faster than negative streamers, but fast negative filamentary streamers have also been observed [18]. Positive streamers can stop during propagation in an inhomogeneous field, which means that inception does not always lead to breakdown. The positive streamer velocity is almost constant during its propagation due to the fact that the streamer is resistive [10].

Streamers have a significant role in the prebreakdown process which thus can be divided into two main events:

1 Streamer initiation

2 Streamer propagation

1.3.6.1 Initiation

• Inhomogeneous fields

The inhomogeneous field may be achieved with a point-plane gap where the plane has a zero potential (not always true).

• Small gaps and AC voltage

The streamers appear when the AC voltage has reached its top value (at the top of the sine wave). The inception probability has an exponential dependence on applied voltage [10]. At low applied voltages, only negative streamers are detected. Positive streamers require about 20% higher voltages to appear at the same probability as the negative ones[10].

• Negative gaps

When the point has a negative polarity, the first visible event is the generation of a microscopic bubble which is preceded by a current burst [10].

• Positive gaps

In positive gaps filamentary streamers occur more often than bushlike [10].

• Small gaps and voltage step

The streamers start to appear within tens of nanoseconds after the applied voltage [9].

• Negative gaps

A local discharge at the cathode produces a spherical gas filled

cavity, which will break up into a negative streamer due to an EHD instability at the surface of the bubble[20].

• Positive gaps

A density change, probably a phase shift, occurs at the tip of the point which will be the initiating event [9].

• Large gaps and AC voltage

The streamers start to appear at about 90% of the top value of the sine wave. Positive streamers have a lower inception voltage than negative [14].

• Homogeneous and semihomogeneous fields

• Small gaps

The initiation of the streamer depends on the design of the electrodes and on the liquid used [15]. Particles in the oil have a significant role since their existence will act as a perturbation on the system which will enhance the probability of initiation. In AC voltage fields it is reported that negative streamers appear more often than positive [10].

1.3.6.2 Propagation

• Inhomogeneous fields

• Small gaps, AC and step voltage

• Negative gaps

The propagation phase has a strong dependence on applied voltage. With a low applied voltage (E < 20 kV/cm, point-plane geometry [10]) no propagation is observed. The preceding bubble expands slightly, detaches and is swept into the liquid [10].

With higher applied voltage filamentary streamers are observed. The streamer length depends on applied voltage. When the field E is above 80 kV/cm all streamers reach the opposite electrode, but in lower fields (E < 40 kV/cm) they might stop while propagating [10].

The propagation of a negative streamer is associated with fast current peaks. The intensity of the current pulses depends on the applied voltage [10]. The velocity of the negative propagating streamer is not constant, it has a minimum when it has reached about half the gap [18].

• Positive gaps

Two types of streamers have been observed, filamentary and bushlike. The bushlike streamer is more rare and occur in very divergent fields [10]. Filamentary streamers has a constant velocity. The positive filamentary streamer can stop during propagation and the length is linearly dependent on applied voltage [10].

The current recorded is constant during the streamer propagation. Superimposed discontinuities can be found [10].

• Large gaps

In AC voltage fields streamers of both polarities are observed. The positive ones are more dominant, since their ability to propagate is much greater than the negative streamers [14]. One main difference with large gaps compared to small is that the propagation field is much smaller in large gaps, the reason for this is unknown.

• Homogeneous and semihomogeneous fields

The velocity of a propagating streamer is in the same range as in the inhomogeneous case. The positive streamer propagates further in the semihomogeneous field than in the inhomogeneous.

1.4 Triggered electric breakdown

A streamer is always initiated by a perturbing event [9]. This perturbation can be the sudden application of a voltage step or an applied AC voltage with fast rise time. However, deterministic perturbations do not exist while using DC voltage, and one has to look for randomly occurring disturbances. This is a great problem for the experimentalists and is probably the main reason why the most used voltage shapes are step and AC voltage. (Working with DC voltage it is possible to accomplish a perturbing event by choosing a strongly inhomogeneous geometry. The strong electric field (E) at the tip of the point (point-plane geometry) can be enough to initiate a streamer.)

The constitution of the liquid is an important parameter, electronic properties of the liquid affect the process. The presence of particles in the dielectric medium can serve as a necessary perturbation. It is important to notice that this perturbation is not fixed in time.

A perturbation fixed in time can be produced by working with a triggering system. One technique often used is to use a spark plug trigger [22]. A discharge circuit is located at one of the electrodes. When the trigger is fired a well defined energy is released into the dielectric medium by a hot spark. One disadvantage with this type of system is that the trigger has a fixed position, it has to be located on one of the electrodes.

However, in a laser triggered system it is possible to locate the trigger wherever you want. The laser trigger is thus more flexible than the spark plug trigger. In a laser triggered gap the necessary perturbation is produced by the formation of a localised plasma, which make the process deterministic (the starting point of the process is fixed in time).

1.5 Laser triggering system

A triggering system for electric breakdown in liquids has been developed by A.Sunesson and L.Walfridsson [21]. The development is part of a co-operative project between ABB Corporate Research and the Department of Physics, LTH. The configuration of this laser triggering system will be described later in this report, see section [2.1].

With help of the laser trigger it is possible to start the breakdown process at a voltage below the usual inception voltage. The process between the laser shot and the actual breakdown is different from the breakdown process that has been described above.

When the laser has been fired, see fig [1.5], a laser pulse of variable energy is focused into the liquid. If the energy is high enough a plasma is created, see appendix [1]. This plasma is hot, which results in vaporisation of the liquid. An expanding gas bubble is formed. After a delay of about 100 microseconds the gap breaks down.

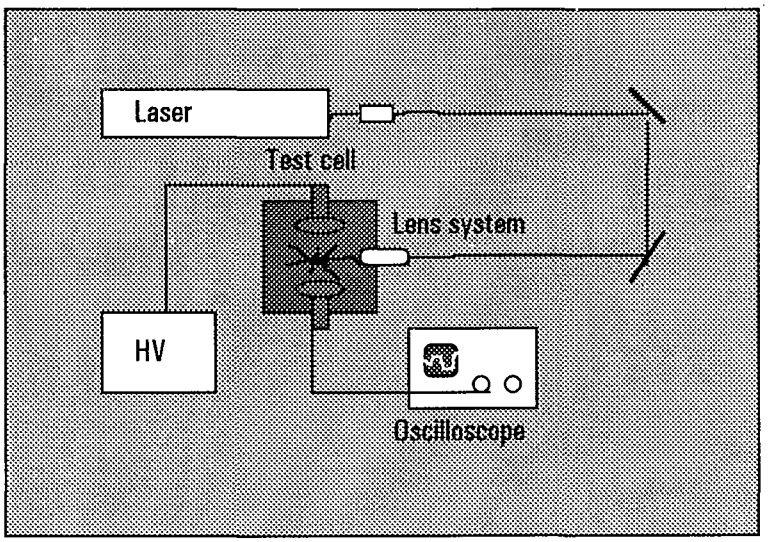

Fig [1.5] Laser triggering system.

1.5.1 EBD versus laser triggered EBD

Although the two processes lead to the same result, the prebreakdown phase is quite different. In the laser triggered case the formation of the plasma is the starting point. In a normal breakdown process the streamer initiation (the starting point) is succeeded by a propagation phase. However, experiments with laser triggered electric breakdown report long delays in time before the gap breaks down. These time lags are too long to be explained solely as streamer propagation, so the phase between the start and the end of the process is quite different in the two cases. Examination of the time lags will be presented further on in this report, see section [4.1].

2 EXPERIMENTAL

2.1 Equipment

The experimental configuration, see fig [2.1], contained several different devices.

A	Laser	G	Photomultiplier
B	Isolator	H	Oscilloscope
C	Mirrors	I	Coaxial cables
D	Lenses	J	Voltage supplies
E	Test cell	K	Power meter
F	Fibre	L	Protection circuit

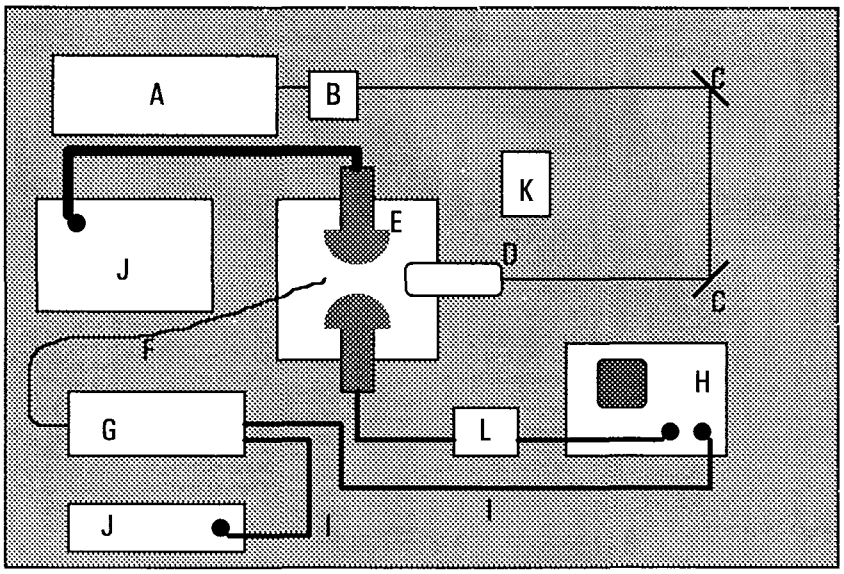

Fig [2.1] Experimental configuration.

A The laser I used was a pulsed Q-switched Nd:YAG laser from Quanta Ray, type DCR-1. This type of laser oscillates at 1064 nm. With help of a doubling crystal it is also possible to extract laser light with two different wavelengths 532 and 355 nm. The pulses that emanate from the laser had a duration of about 10 ns and a variable pulse energy. The energy range was from 0 to 600 mJ/pulse for infrared light. I only used infrared light.

B In order to protect the laser from backscattered light, an optical isolator was placed right after the laser. Backscattered radiation would otherwise reenter the laser and then be amplified. Such amplified laser pulses could damage the laser. The fact that the isolator only permits passage of light in one direction is explained by the rotation of polarisation. When the laser beam enters the isolator it is linearly polarised in one direction. The polarisation axis is then rotated 90 degrees, thus the light in the opposite direction can not pass the first polarisator.

C The mirrors used were selected to operate in the IR range. When the light had a wavelength of 1064 nm the mirrors reflected 99% of the light.

D A lens system focused the laser beam into one spot between the two electrodes. In choosing the lenses, it is necessary to take into account the problem of self focusing and spherical aberration [21].

E The vessel that contained the dielectric liquid is called the test cell. The cell was cube shaped and had four thick windows. The two electrodes are pointing out from the other two sides, see fig [2.2].

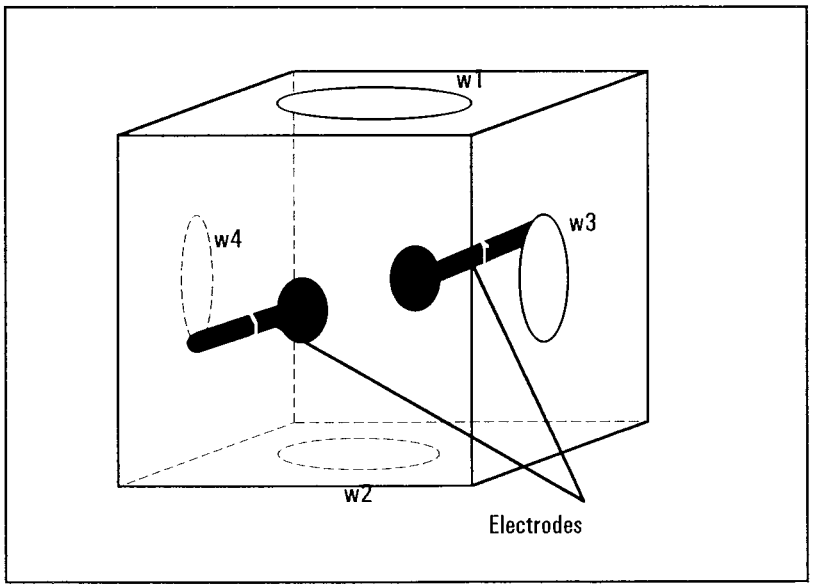

Fig [2.2] Four windows on test cell.

The electrodes are made out of brass and are hemispherical, see fig [2.3]. They have a radius of curvature of 10 mm. The separation of the electrodes is variable and is called the gap length. One of the windows is placed inside the test cell, see fig [2.4], which makes it possible to place the focusing lens system closer to the electrode gap.

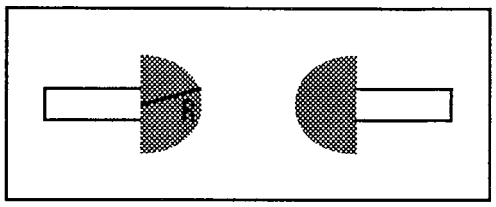

Fig [2.3] Hemispherical electrodes, R=10mm.

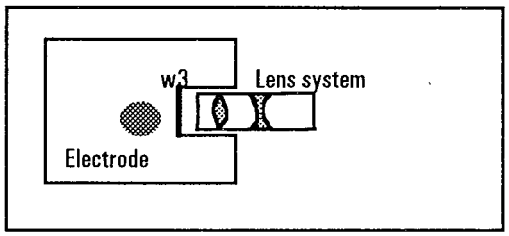

Fig [2.4] The lens system is close to the electrodes.

F The optical fibre used had a diameter of 0.6 mm.

G I have used two different photomultipliers, EMI-6256 and EMI-9558B, see appendix [2]. The first photomultiplier was chosen because it had a very high gain and could therefore be used for photon counting. The second photomultiplier is the one that has been used in most of the light measurements. It has a low dark current, high gain and fast rise time (10 ns). The terminology will be explained further on in this report, see section [2.2].

H The oscilloscope used was a Tektronix TDS-540. It is a digital oscilloscope with 1 GHz sampling rate and an analogue bandwidth of 500 MHz. Using only one channel on the scope, it was possible to make one billion samples per second. I was able to communicate with the oscilloscope through a GPIB cable with a connected computer. This ability made it easy to store interesting data on file, which was a great

help.

I Some of the coaxial cables I used (between the photomultiplier and the oscilloscope and between the photomultiplier and the voltage supply for the PMT, see fig [2.1]) in the experimental set-up were shielded four times to prevent disturbances that could influence the measurements. These cables were very stiff and were hard to handle.

J Two voltage supplies were used, one for the photomultiplier and one for the test cell. The high voltage (HV) for the test cell was delivered by a FUG capable of delivering +/- 65 kV. For security reason it was fused to prevent current flow exceeding a pre-set maximum level. If the current level was exceeded the FUG would automatically shut down. The voltage supply for the photomultiplier was an Oltronix A3.4K-40R.

K A integrating power meter named Schientech ASTRAL AA30 was used to measure the pulse energy.

L In order to protect the oscilloscope from too high voltage level during breakdown, a protection circuit was installed between the test cell and the scope. The bandwidth of the circuit was 700 MHz. The protection circuit removes voltage levels and transients above 1.5 V amplitude.

2.2 The first configuration

The first two months of the diploma work was spent on developing a control device for the photomultiplier. In the beginning it looked very promising but in the end I had to abandon this method due to great electric disturbances.

2.2.1 The photomultiplier

In order to detect very faint light, photomultipliers are used. In a photomultiplier (PM-tube) dynodes are placed in a chain with increasing potential. The dynodes are coated so that they have a high secondary emission coefficient (δ); consequently several secondary electrons are emitted from the surface of the dynode for each impinging

electron. When a photon hits the cathode one or more photoelectrons are emitted. These electrons are accelerated to each succeeding dynode in the chain, where further amplification occurs.

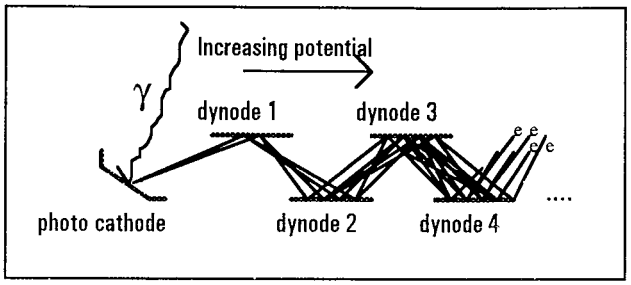

Fig [2.5] Chain of dynodes.

The resulting current from one impinging photon is determined by the secondary emission coefficient and the voltage applied over the dynodes. If the chain of dynodes consists of n numbers of dynodes the amplification factor will be in the region of δ^n. Usually n lies between 10 and 13, which gives an amplification factor of the order of 10^6.

The voltage U applied to the chain of dynodes is an external variable parameter.

The advantage with a photomultiplier is:

- High sensitivity - The large gain (amplification factor) makes the photomultiplier extremely sensitive to light. If the gain is high enough it is possible to detect single photons.

- Low noise - Every amplifier is attached to a certain amount of noise. The noise in a photomultiplier is very low compared to other amplifiers such as a photo diode for instance.

The photomultiplier must be treated with great care. Too much light can literally set the PM-tube on fire. It is therefore of utmost importance not to exceed the upper current limit, indicated by the manufacturers. This upper limit will set a standard for how much light the photomultiplier can take. This limit is for continuos light. Therefore, single pulses that exceed the upper limit will not destroy the PM-tube.

Another feature of the photomultiplier worth mentioning is the phenomenon called 'blindness'. If a PM-tube receives to much light during a short period of time the qualities of the photomultiplier can change. The dark current and the noise are raised, the light sensitivity is reduced, imaginary pulses can occur after the big pulse and a remaining false signal can last for up to tens of microseconds. It can take a long time for the photomultiplier to recover ranging from a couple of hours up to days in the worst case.

2.2.2 The configuration

The light emitted during a laser triggered electric breakdown has a specific appearance, see fig [2.6].

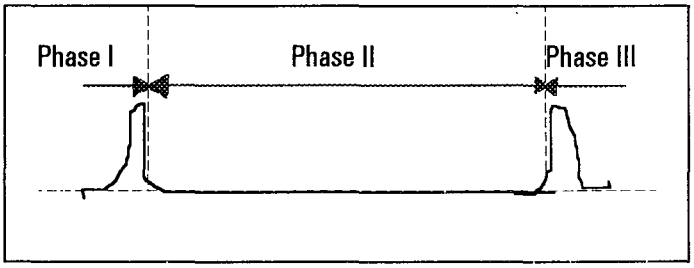

Fig [2.6] Schematic view of light recorded with a photo diode.

Three different phases can be distinguished. Phase one starts when the laser pulse hits the liquid. If the intensity in the focal spot is high enough a plasma is created. This plasma will burn about hundreds of nanoseconds. Phase one ends when the plasma fire is extinguished. Phase two constitutes of a long delay before breakdown. Phase three is the actual breakdown.

In both phase one and three very strong light is emitted during a short period of time.

As mentioned above, I was to make measurements from the light emitted during the prebreakdown events, i.e. during phase two. This created a practical problem. How would I be able to measure light during phase two, without making the photomultiplier 'blind' by the

very strong light pulses? The best would be to make the photomultiplier sensitive only during phase two. The risque of 'blindness' would then have been eliminated.

This is the reason why I tried to develop a gating device for the photomultiplier. When using the word gate, it means a possibility to control when the PM-tube should be sensitive and for how long.

The following system was developed, see fig [2.7].

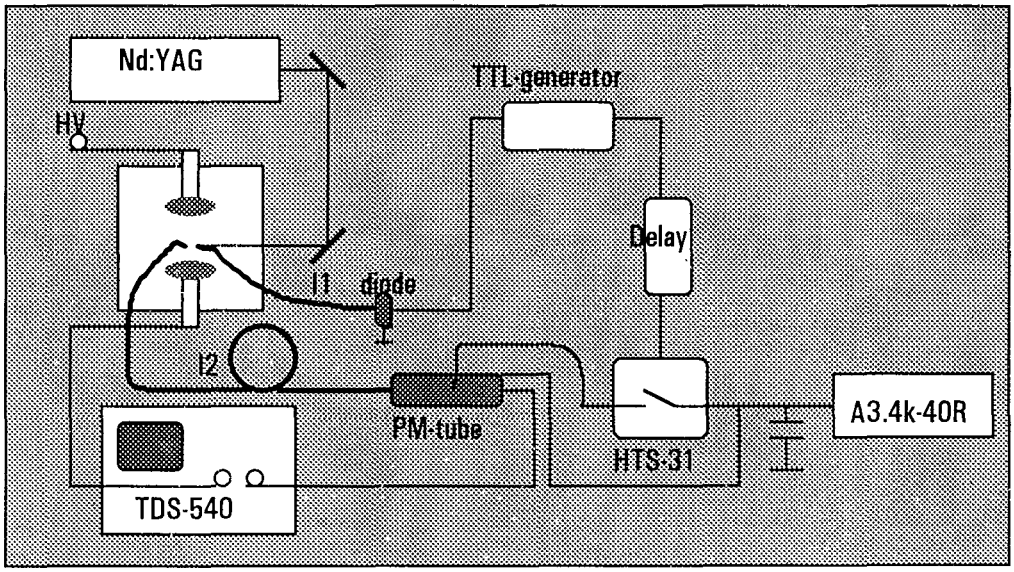

Fig [2.7] Experimental configuration.

Two optical fibres of different lengths were placed in the gap. This difference in length made it possible to see what you were going to see before you actually saw it! An optical delay T_O can be calculated

$$T_O=(l_2-l_1)/c \qquad [2.1]$$

where c is the speed of light. This optical delay was used in the system. It will take T_O seconds for the light to reach the photomultiplier after it has reached the diode. The TTL-generator creates a TTL-pulse which is high during phase two, see fig [2.8].

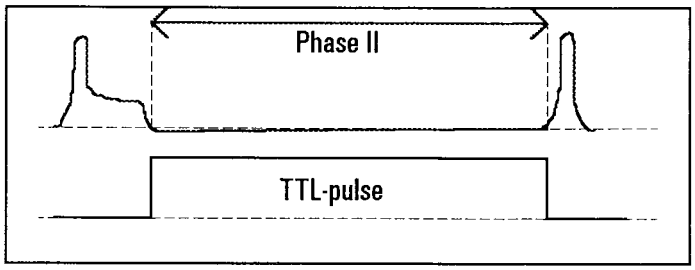

Fig [2.8] The upper trace is the light received by the diode.
The lower trace is the output signal from the TTL generator.

The logic pulse is then retarded t_0 seconds in an electrical delay. This pulse controls the high voltage switch, HTS-31. The switch delivers high voltage to the photomultiplier as long as the control signal is high, see fig [2.7].

With the variable delay t_0 in the electrical delay, it is possible to set the photomultiplier in active mode when the second phase reaches the PM-tube. This is done by choosing t_0 as

$$t_0 = T_0 - t_{TTL} - t_{DELAY} \qquad [2.2]$$

where t_{TTL} and t_{DELAY} is the electric transit time in the TTL-generator and the electrical delay. During phase one and three the PM-tube is not in an active mode, which makes it not sensitive to strong light.

2.2.3 The modification of a photomultiplier

The photomultiplier I tried to modify was an EMI-6256, see appendix [2]. It consists of four main components.

1 The tube - All the dynodes and the photocathode are placed here. The tube is connected to the socket through 15 pin connections, see fig [2.9].

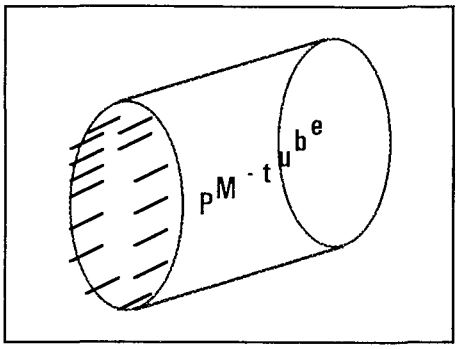

Fig [2.9] 15 pin connections at one side of the tube.

2 The socket and the voltage divider- All other electrical components such as resistors and capacitors were placed here. The socket is usually filled with an insulating material. At the bottom of the socket there are two connectors. One is for the high voltage supply, the other is for the emanating anode current. The socket is connected to the envelope.

3 The envelope - To secure that no light can penetrate the joint between the socket and the envelope, O-rings are used. The envelope covers the tube. The envelope I used was made out of aluminium and was constructed at the workshop of LTH, Department of Physics.

4 The light was led through an optical fibre which was connected to the end of the envelope with help of a fibre connection, see fig [2.10].

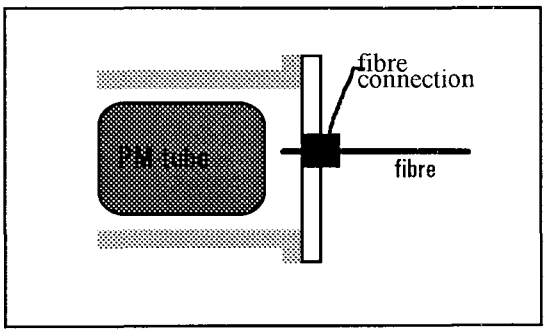

Fig [2.10] Fibre connection.

A photomultiplier can schematically be described like this:

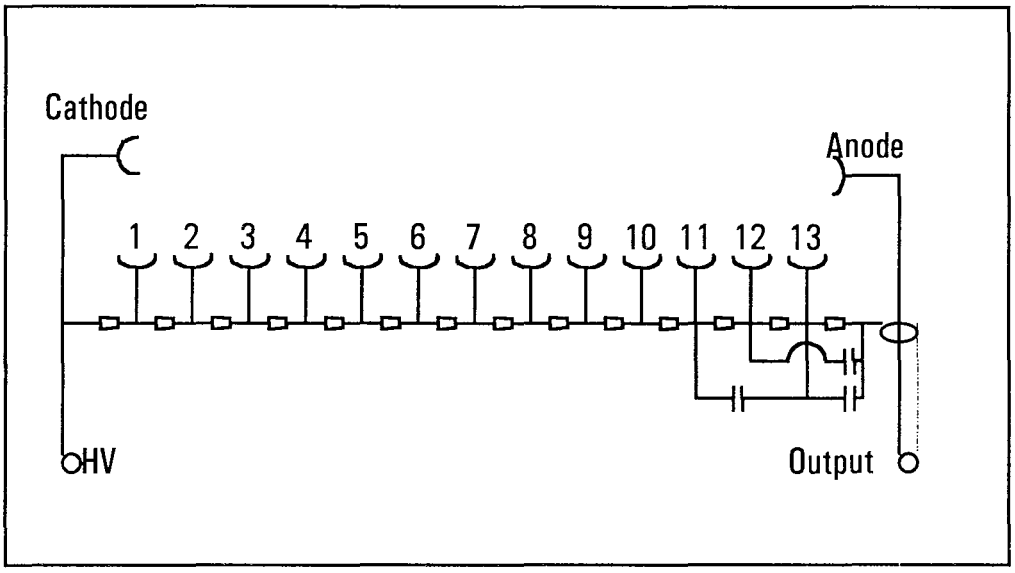

Fig [2.11] Voltage divider with 13 dynodes.

The voltage divider, a series of resistors, delivers an increasing potential to the respective dynodes. The potential ascends from -HV to 0 volts.

If the applied voltage is suddenly altered from 0 to -HV, big transients will be transferred down the voltage divider and it will take a while until the system restores its stability. Therefore a change in the construction of the PM-tube was inevitable.

After many experiments where the potential of the dynodes was measured as a function of time and a lot of practical work such as soldering, the final configuration looked like fig [2.12].

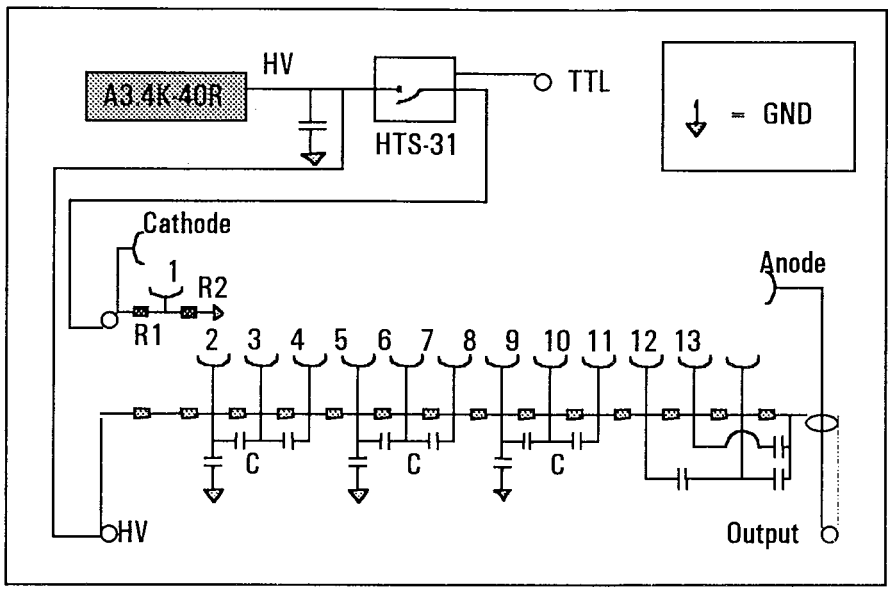

Fig [2.12] The voltage is connected at two different connections.
R1=154Ω, R2=839Ω, C=0.1μF

The possibility to modify the electric circuit was arranged by the use of an extender, see fig [2.13].

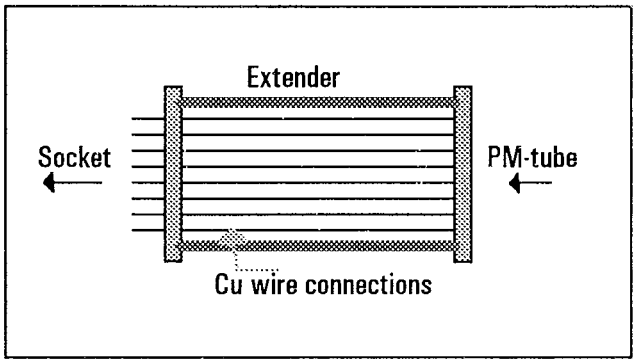

Fig [2.13] Extender

By leading current directly to the extender, and not through the socket, it was possible to switch chosen parts of the chain of dynodes.

Capacitors were added to reduce transients.

By only switching the voltage over the photocathode and the first dynode several advantages were achieved:

1 Before applying the high voltage pulse, the dynodes 2 to 13 have the right potential, see fig [2.14]. The photo cathode and the first dynode have a zero potential which makes the system insensitive to light. The explanation to this is simply that the photo emitted secondary electrons are not accelerated along the chain of dynodes.

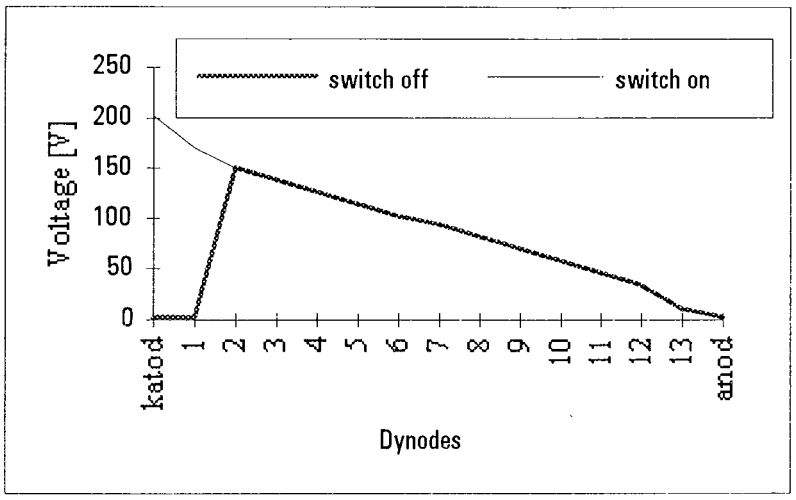

Fig [2.14] Potential of the dynodes.

2 When calculating the time for the system to stabilise, it was not necessary to take into account the capacitors in the end of the voltage divider. This improved the response time for the system.

2.2.4 Discussion

Measurements of the potential of the dynodes as a function of time showed that the modified photomultiplier worked as expected. When the light from phase 2 reached the PM-tube every dynode had a stable and correct potential.

Now I thought that I had reached the end of the first stage of my work. Design, construction and testing was finished and done.

2.2.5 Disturbances

The results of the measurements of emitted light from breakdown events, performed with the modified photomultiplier, was not as expected. They did not contain any pulses correlated with the current. Only noise was detected.

Several different techniques, to reduce these disturbances, was tried, the use of a common ground and shielding of the coaxial cables for example. None of these attempts was successful enough. To make a long story short, you can say that the extender and the envelope, more or less, was working as a noise receiver. The conclusion was that accurate measurements could not be made with this system!

2.2.6 An idea

It was at this point I tried to connect the PM-tube (EMI-9558) to a continuous voltage source. It worked! The disturbances were almost gone and I received a distinct light trace. It appeared that the risque for 'blindness', discussed above, was most exaggerated. The strong light pulses did not affect or damage the photomultiplier. The noise was lower here due to a better envelope. The experimental configuration was found, see fig [2.1]!

2.2.7 Summary

There are three reasons why this 'mistake' has been described in the report.

1 The development of the system took a long time.

2 There are alternatives for this type of system on the market, multi channel plates for instance. However, they are very expensive. With further development, this system might be a low cost alternative!

3 I learned a lot about practical trouble shooting and electrical engineering through this initial work.

3 RESULTS

In all my experiments described below, I used a transformer oil (NYTRO 10 X) at room temperature, as insulating liquid. It is a commercial oil manufactured by NYNÄS, with a relative permittivity of $\varepsilon_r = 2.2$ and a density of $\delta = 872$ [kg/m^3]. The liquid was not filtered during the experiments.

3.1 Spontaneous breakdown

It is well known that the spontaneous breakdown is preceded by streamer propagation. Therefore, series of measurements of spontaneous breakdown were made to look for characteristic features that could be compared with measurements from triggered breakdown. These experiments were difficult to perform, since breakdown often occurred before the applied voltage was stable. A characteristic measurement can be seen in fig [3.1].

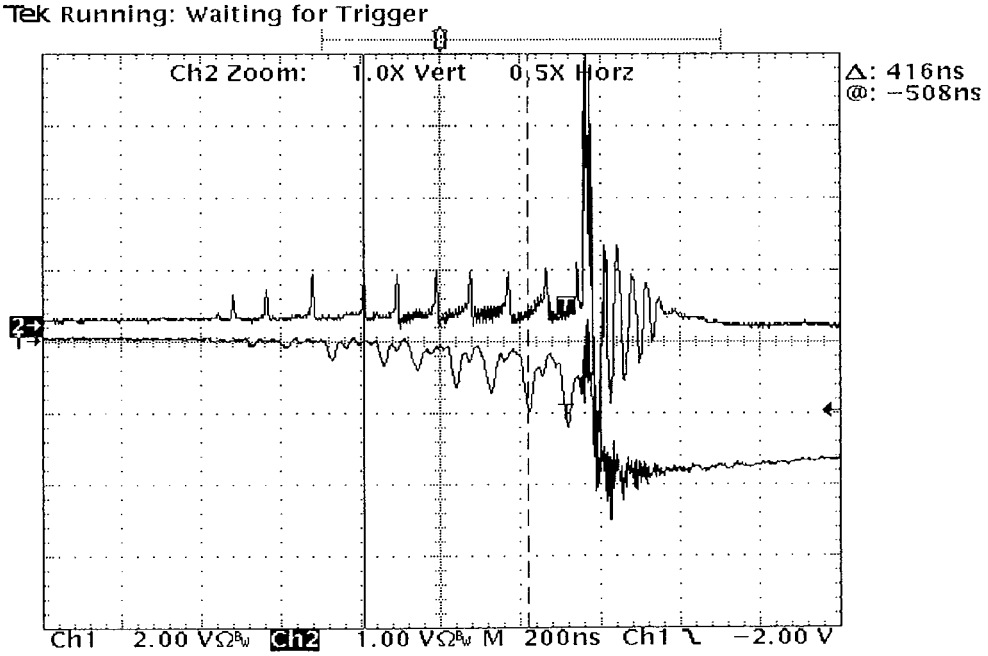

Fig [3.1] CH1 is light, CH2 is current, applied voltage is +59 kV

The light pulses are displaced relative to the current pulses in time by a constant factor, T_D. This is due to the fact that the passage through the photomultiplier takes a certain amount of time. The PM-tube EMI-9558 has an electron transit time of about 65 ns, see appendix [2]. The transit time equals the constant T_D, therefore the light and the current pulses are correlated in time.

The following statistics were collected. Introduce U,T and N where

U - is the voltage applied to the test cell.
T - is the time between the first pulse and the breakdown.
N - is the number of pulses before breakdown.

U [kV]	T [µs]	N [#]
57,0	0,86	10
59,3	0,77	9
60,1	0,64	7
62,7	0,852	9
64,8	1,03	10
65,0	0,72	6
-65,0	0,89	9
-63,9	0,85	10
-62,8	0,89	9

Tab [3.1] Spontaneous breakdown

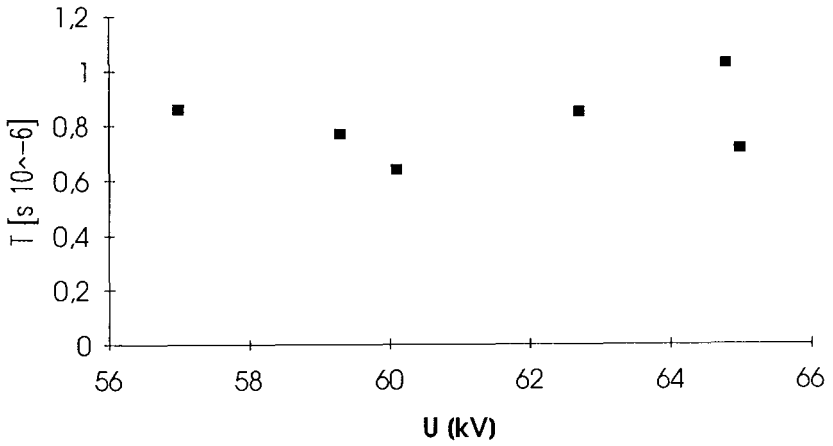

Fig [3.2] Time to breakdown

From the measurements of spontaneous breakdown, it is hard to derive any general conclusions. A few remarks can be done, though.

1 The spontaneous breakdown constitutes of two parts; a prebreakdown phase and the actual breakdown.

2 The prebreakdown phase is about 1 microsecond and consists of about 10 well correlated light and current pulses.

3 The continuous component of light, as can be seen in fig [3.1], might be due to the fact that the PM-tube does not have time to recover from one light pulse to the other.

3.2 Variables

To understand a physical problem it is important to know which parameters that are influencing the process and how they do it. While studying a phenomenon it is therefore important to extract the governing variables. This can be done with dimensional analysis and 'physical intuition'. If one chooses wrong parameters these can soon be excluded, because wrong variables will not affect the process.

In a laser triggered breakdown there are many parameters that could influence the process. Two classes can be distinguished; outer and inner parameters:

- outer variables are quantities that are put into the system such as laser pulse energy and applied high voltage and
- inner parameters are quantities that define the system, such as gap length, test cell geometry, electrode shape etc. These parameters have one thing in common, they all affect the electric field.

I have chosen to work with two outer parameters:

1 applied voltage,

2 laser pulse energy

and one inner parameter

3 location of focal spot.

The location of the focal spot is an inner parameter since the creation of space charge will affect the electric field. I have also tried to restrict the collected light by changing the fibre position.

3.3 Triggered breakdown

The laser triggering process has shortly been described above, but I think it is necessary to further develop the concepts before proceeding.

The plasma formation is the initial process. It is accompanied by shock waves and bubble formation, which can be heard as a distinct sound. Then there is a long time delay before breakdown ranging from tens to hundreds of microseconds before breakdown. The delay can be divided into two parts; before and after 'the large pulse', see fig [3.3].

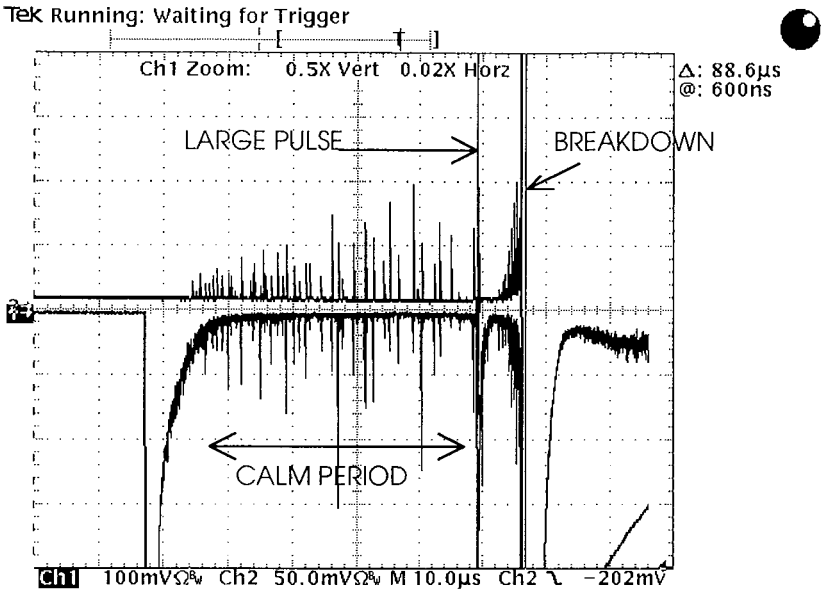

Fig[3.3] A large pulse can be seen 50 µs after the laser pulse
Applied voltage is +35 kV, laser pulse energy is 200 mJ

In almost every laser triggered breakdown a large pulse can be seen before breakdown occurs. The pulse is much larger than the rest of the pulses but not as large as the actual breakdown.

- **Calm period** - The period before the large pulse will be denoted as the calm or the low active period and constitutes of occasional distinct pulses. No continuous components can be found. See fig [3.3].

- **Intense period** - The time interval between the large pulse and the breakdown varies. If the time before the pulse can be denoted as calm, the time after the pulse is best depicted as intense. Many rapid pulses, sometimes superimposed on a continuous component, can be seen. The amplitudes of the pulses seem to grow in time. See fig [3.4]. This part of the process might be streamer propagation.

The process is terminated by an electrical breakdown.

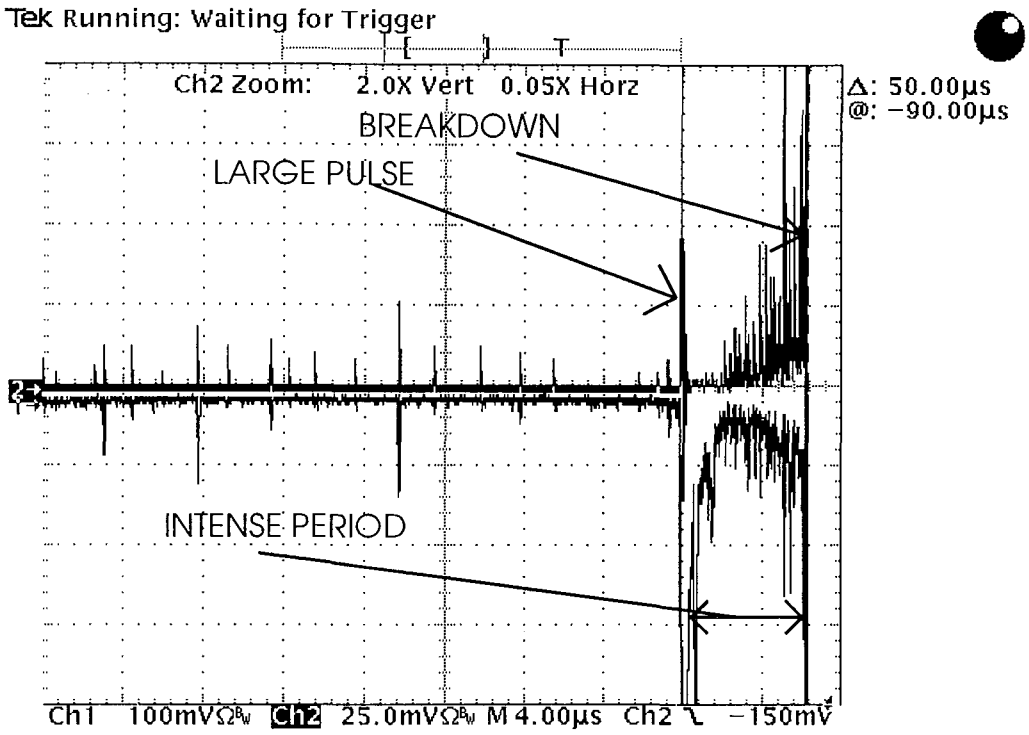

Fig [3.4] Applied voltage is +50 kV, laser pulse energy is 100 mJ.

3.4 Applied voltage

I have made measurements with different applied voltages when the other variables were held fixed. The voltage was delivered by a FUG as mentioned above. The fuse mechanism, which automatically shuts down the FUG when the current flow is too high, produced a practical problem. If the pulses right before breakdown is high enough, they will trigger the fuse, and the FUG will shut down. Therefore a big capacitor was placed between the high voltage electrode and the grounded shell of the test cell. This capacitor was capable of delivering the charge necessary to complete the breakdown.

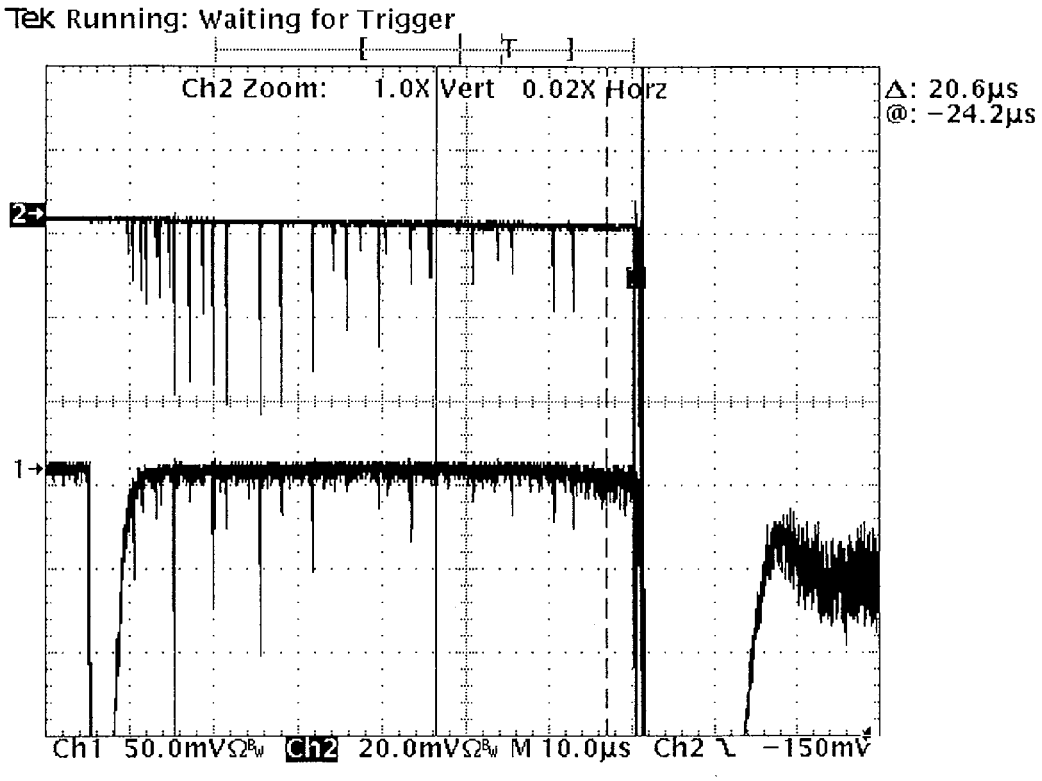

Fig [3.5] Applied voltage is -30 kV, laser pulse energy is 100 mJ.
CH1 is the light and CH2 is the current.

In the experiments described below, the position of the focal spot will be in the middle of the gap. Some characteristic measurements can be seen in fig [3.5, 3.6].

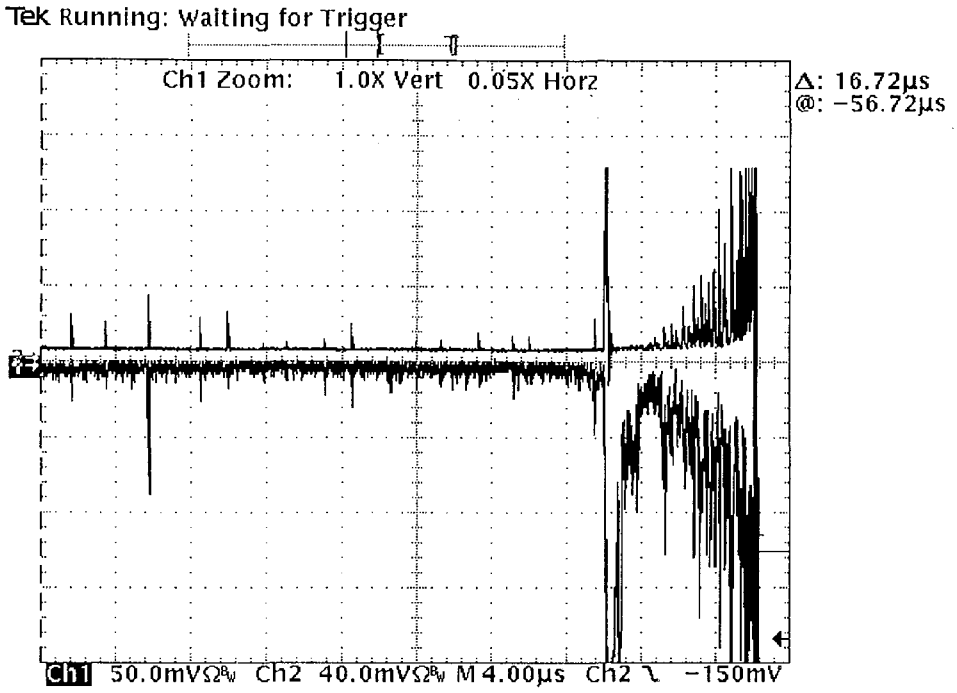

Fig [3.6] Applied voltage is +50 kV, laser pulse energy is 100 mJ.
The upper trace is the current and the lower is the light.

Let the breakdown process be described by the following parameters.

U - Applied voltage
T_{BD} - The time between the trigger event and the breakdown
T_{LP} - The time between the large pulse and the trigger event
ΔT - $\Delta T = T_{BD} - T_{LP}$
N_{BLP} - The number of pulses before the large pulse
N_{ALP} - The number of pulses after the large pulse
n_{BLP} - $n_{BLP} = N_{BLP} / T_{LP}$
n_{ALP} - $n_{ALP} = N_{ALP} / \Delta T$

The following statistics have been collected, see fig [3.7 → 3.15]. Five different samples were collected at each voltage level.

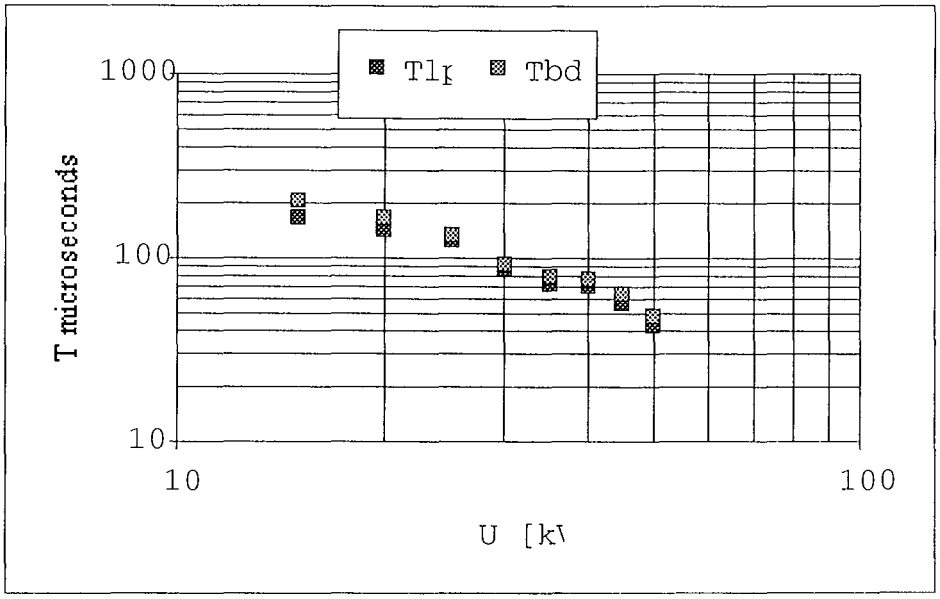

Fig [3.7] Tlp and Tbd is measured as a function of voltage.

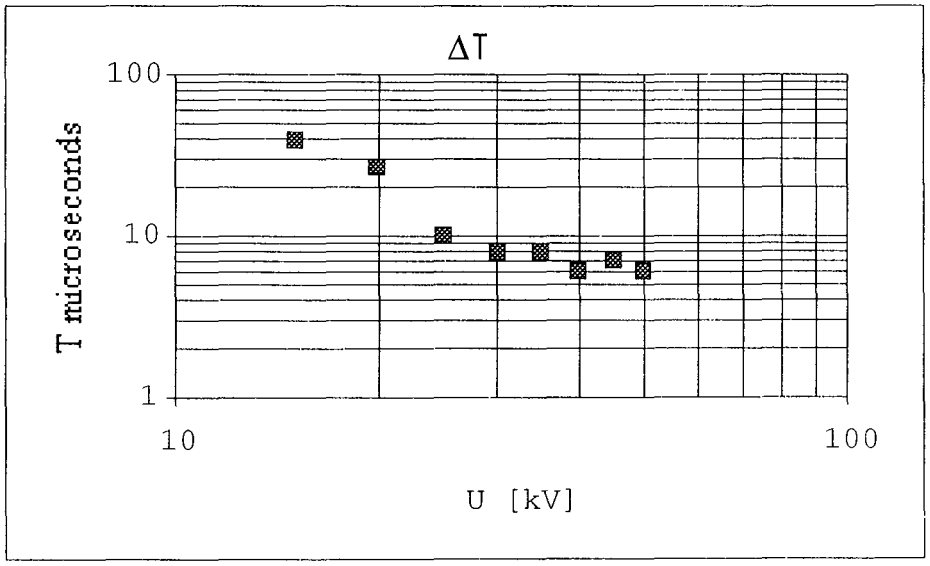

Fig [3.8] ΔT as a function of applied voltage.

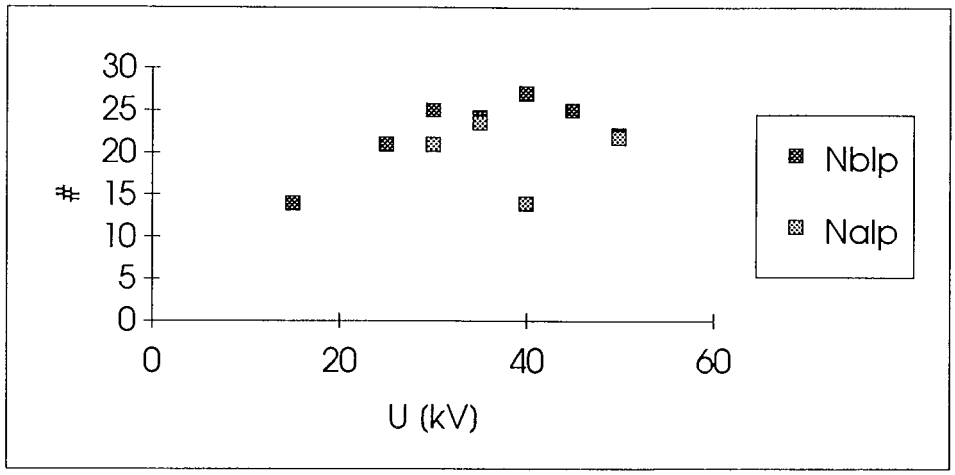

Fig [3.9] The number of pulses, before and after the large pulse

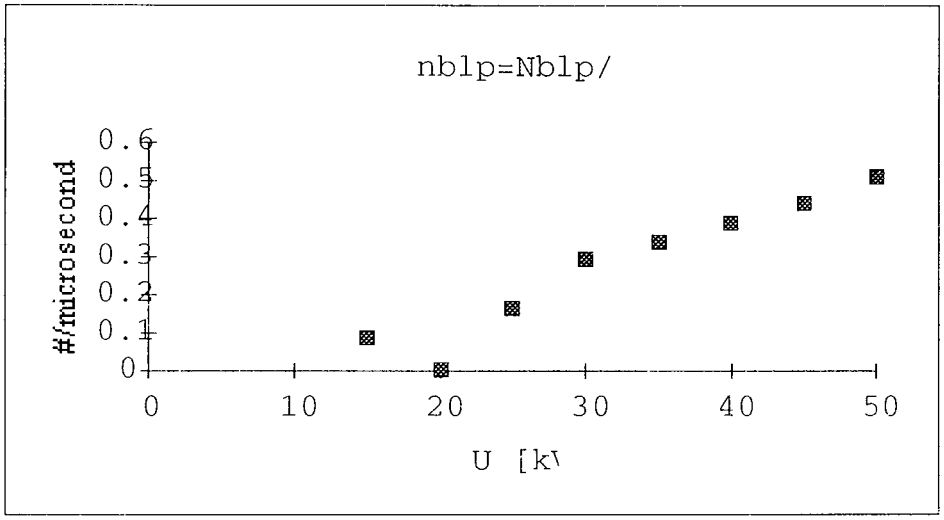

Fig [3.10] Pulse density before large pulse.

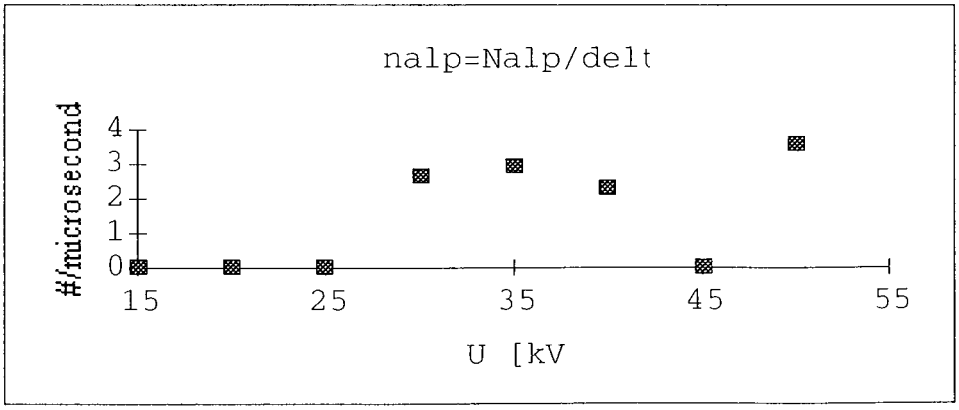

Fig [3.11] Pulse density after large pulse

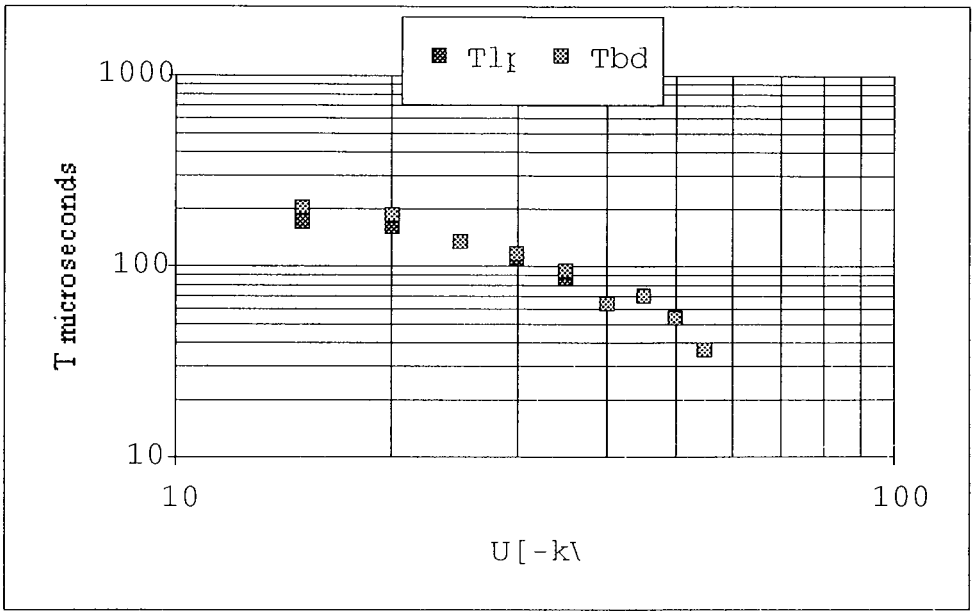

Fig [3.12] Time lags in negative applied voltage.

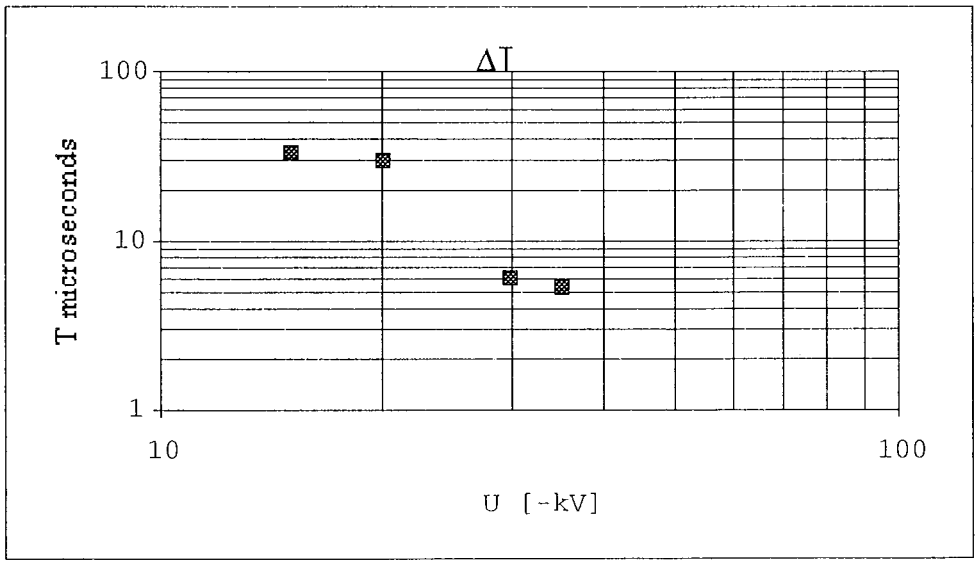

Fig [3.13] ΔT in negative applied voltage.

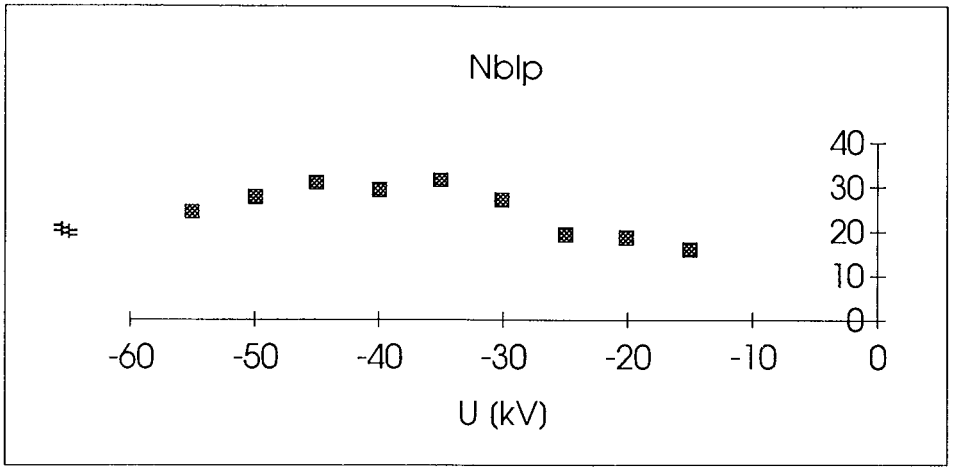

Fig [3.14] The number of pulses before the large pulse.

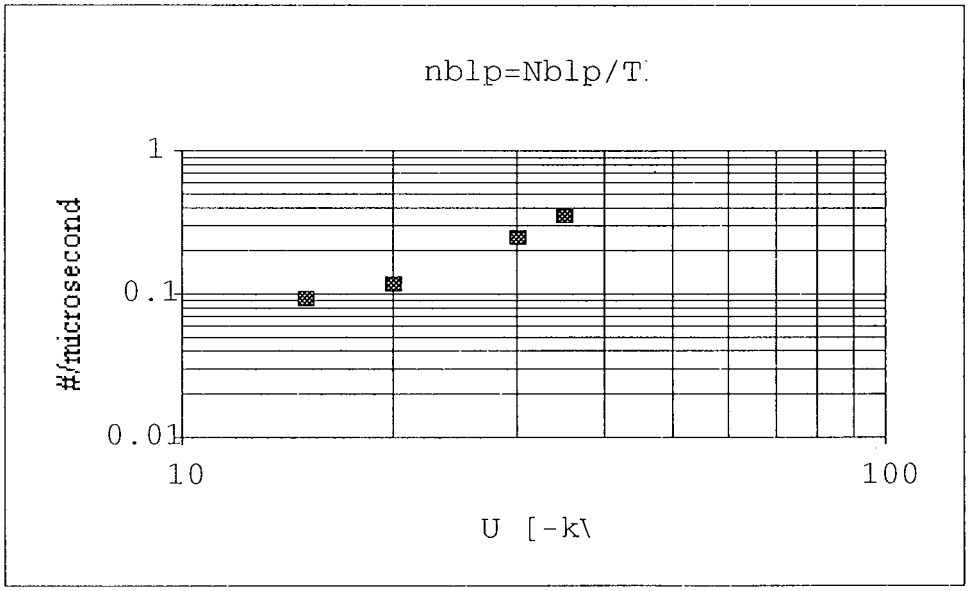

Fig [3.15] The pulse density before the large pulse.

A few remarks are to be noticed:

- There seems to be an exponential relation between the time lags and the applied voltage, as can be seen in fig [3.7] and fig [3.12].The time to breakdown decrease as the voltage (|U|) rise.
- The large pulse can not be seen if the voltage is below -35 kV in the negative polarity case, see fig [3.12].

- The time between the large pulse and the breakdown (ΔT) decreases as the voltage is raised. There seems to be an exponential relation, see fig [3.8] and fig [3.13].
- The pulse density seems to increase linearly when the applied voltage is raised (positive polarity), see fig [3.10]. In negative polarity the pulse density seems to have an exponential dependence of applied voltage, see fig [3.15].

3.5 Pulse energy

The laser pulse energy is variable. I made series of measurements with different pulse energies when the applied voltage was held constant (+25 kV). During the experiments, the focal spot was placed in the middle of the electrode gap. The energy is measured before the pulse enters the lens system. A characteristic measurement can be seen in fig [3.16].

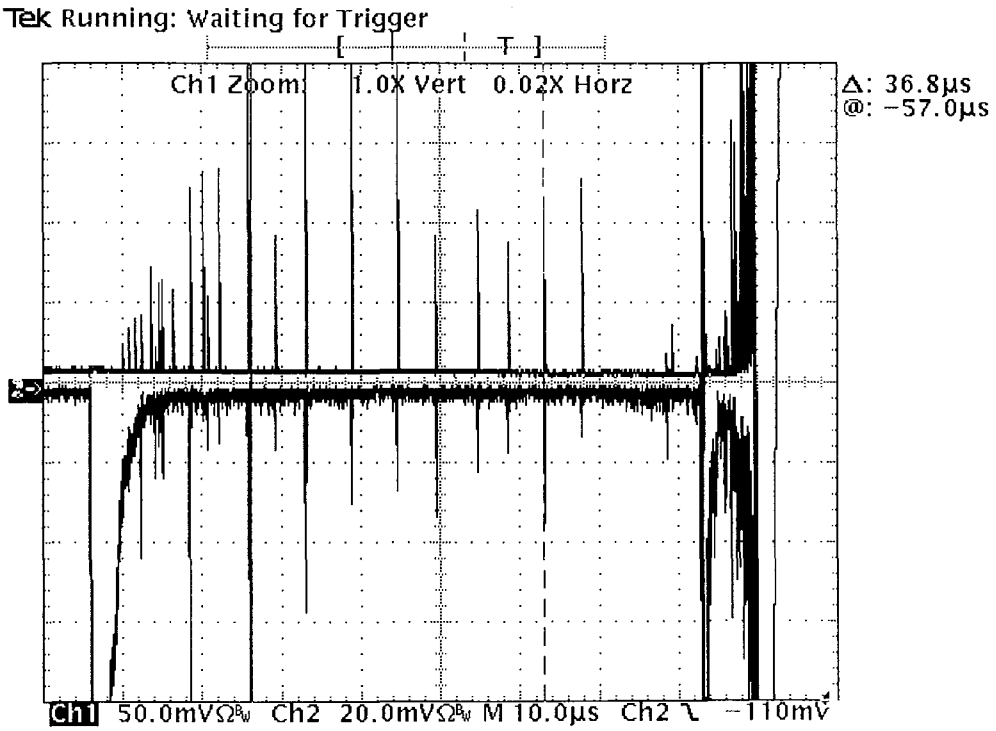

Fig [3.16] Applied voltage +25 kV, laser pulse energy 100 mJ
Upper trace is current and lower is light.

Three different time lags were measured during the experiments, time to large pulse (T_{lp}), time to breakdown (T_{bd}), and their difference ΔT ($\Delta T = T_{bd} - T_{lp}$). Ten different samples were made at each energy level. The focal spot is placed in the middle. The time between the initial triggering event and the breakdown is dominated by the calm period, as can be seen in fig [3.17].

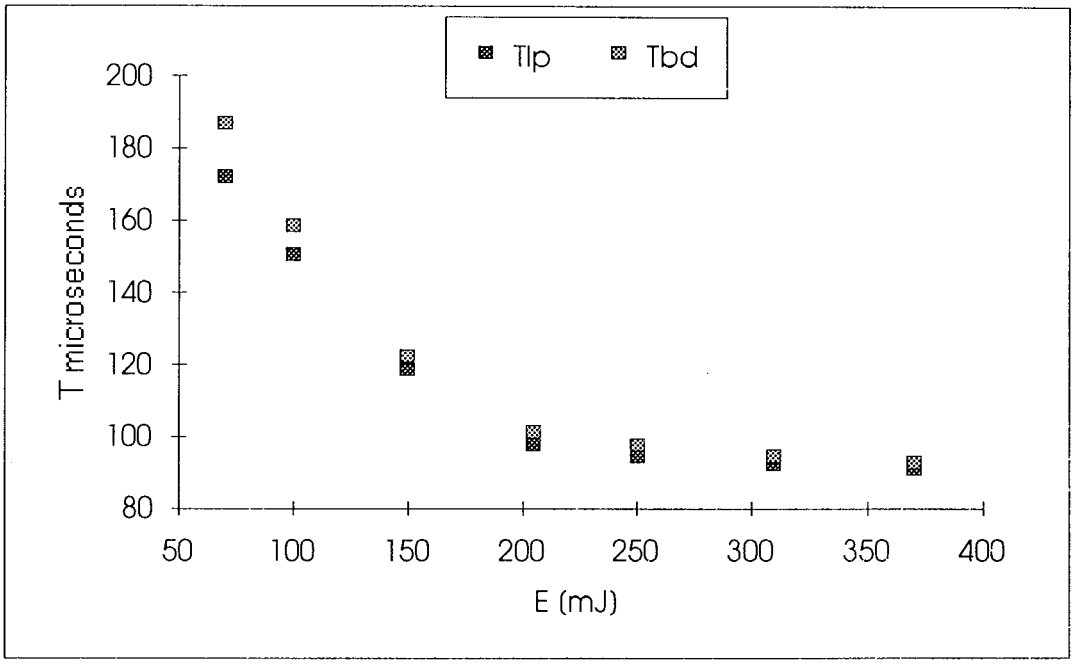

Fig [3.17] Time lags as a function of energy.

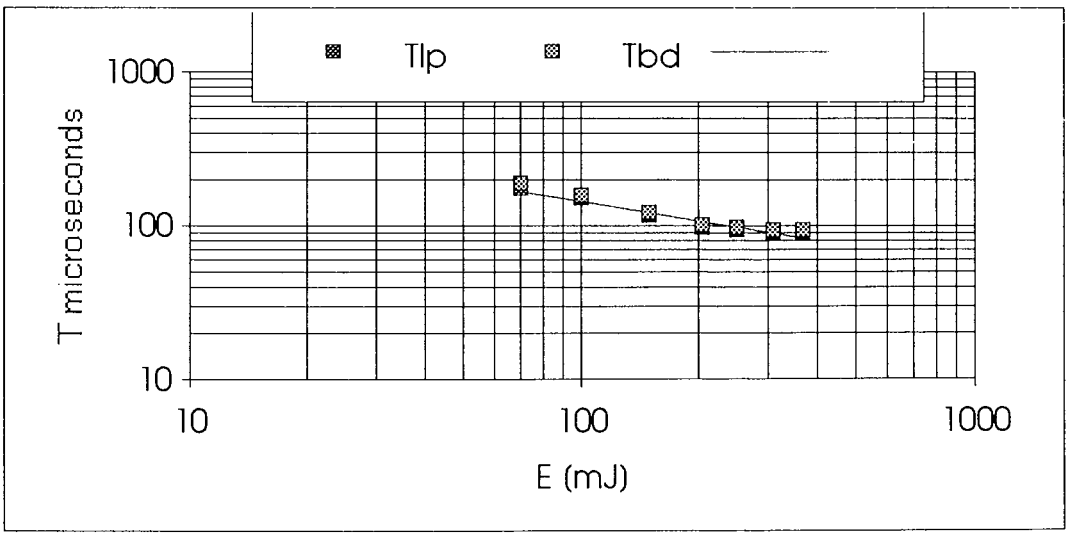

Fig [3.18] The same plot as in fig [3.17].

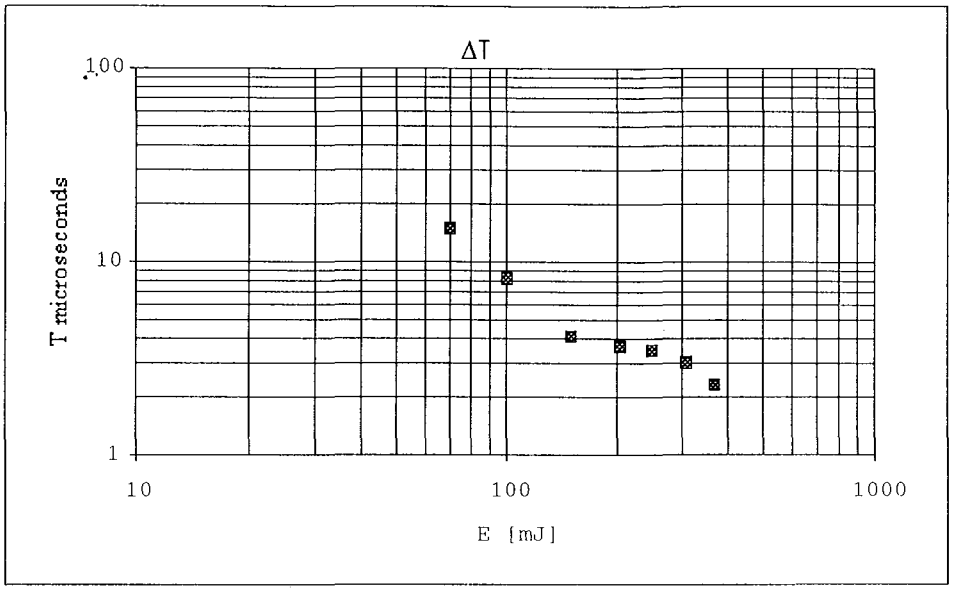

Fig [3.19] ΔT as a function of laser pulse energy.

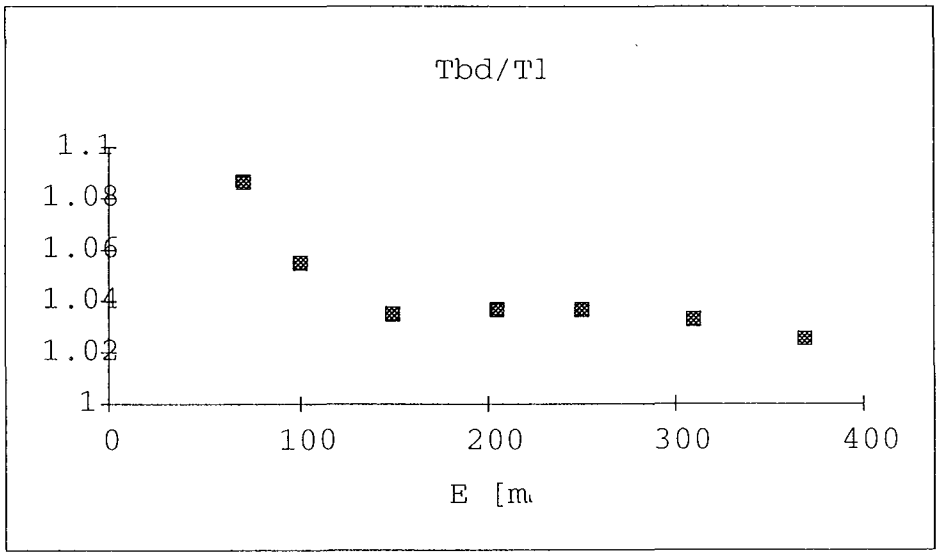

Fig [3.20] Relation between Tbd and Tlp.

This is not always true though, see next section. The relation between time to the large pulse and time to breakdown is almost constant and does not seem to depend on energy, at least above E=150 mJ, see fig [3.20]. By choosing pulse energies above (E > 200 mJ), where the dependence on energy cease, the time delay can be minimized. As can be seen in fig [3.19] ΔT seems to have an exponential dependence on laser pulse energy.

3.6 Focal spot position

In order to investigate how the laser triggered breakdown process was affected by the position of the focal spot, two series of measurements were made. The applied voltage was +/- 40 kV. The electrode gap was divided into eight equal distances (0.625 mm) to be able to locate the focal spot at nine different positions (pos1...pos9). Position 1 was located outside the ground electrode and position 9 outside the high voltage electrode, see fig [3.21].

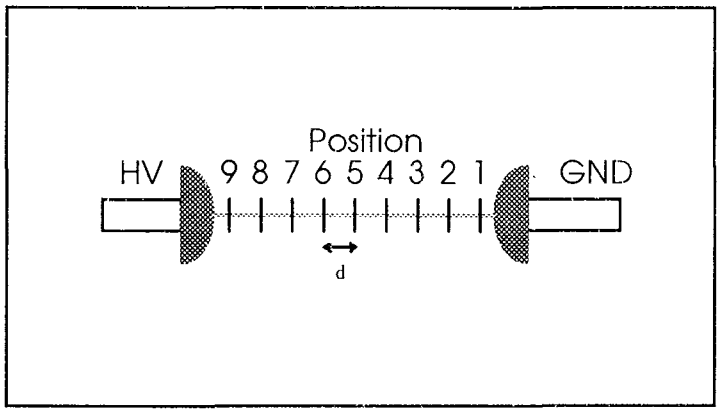

Fig [3.21] Focal spot positions, d=0.625 mm.

Three different time lags were measured; time to the large pulse T_{lp}, time to the breakdown T_{bd} and the difference $\Delta T=T_{bd}-T_{lp}$. Ten different samples were made at each focal spot position. The results are shown in fig[3.23...3.25]. A characteristic measurement is seen in fig[3.22].

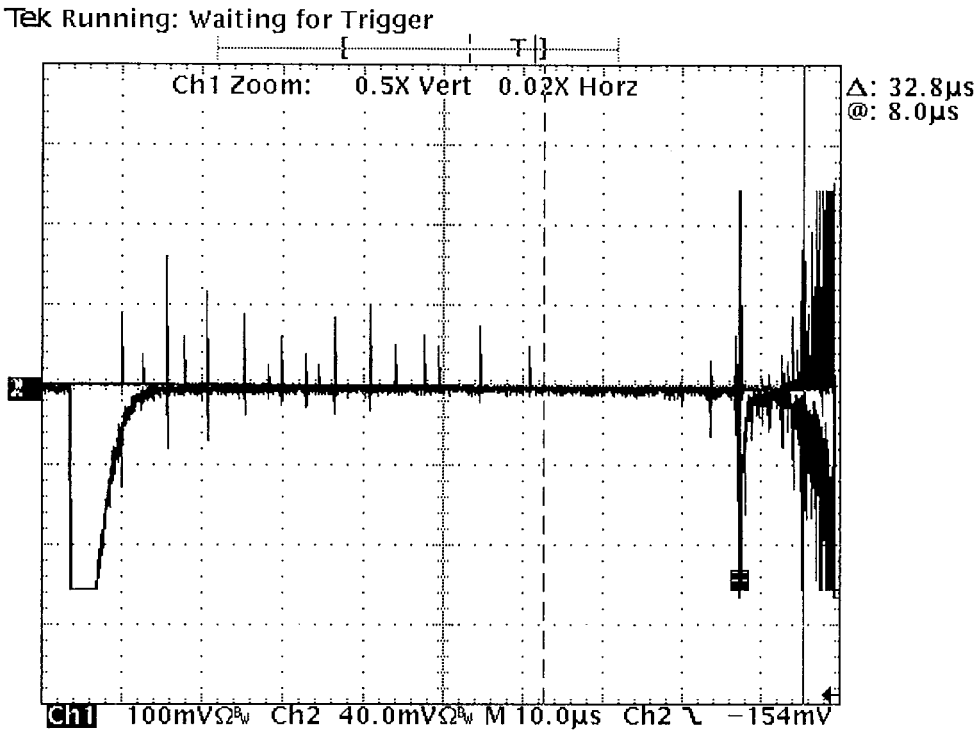

Fig [3.22] Applied voltage is +40 kV, laser pulse energy is 165 mJ.
Focal position is pos 4.

As can be seen in fig [3.23] T_{LP} has a maximum when the focal spot is in the middle of the gap. If the large pulse is the result of a connection between the bubble and the electrode, the maximum in T_{LP} implies that this connection is made to the closest electrode.

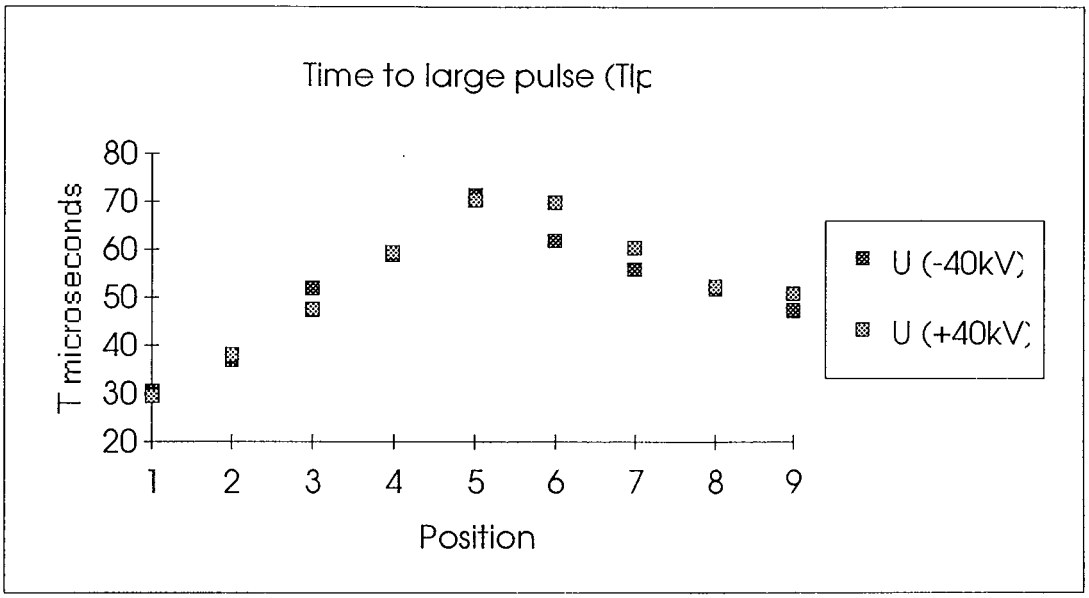

Fig [3.23] Tlp as a function of position.

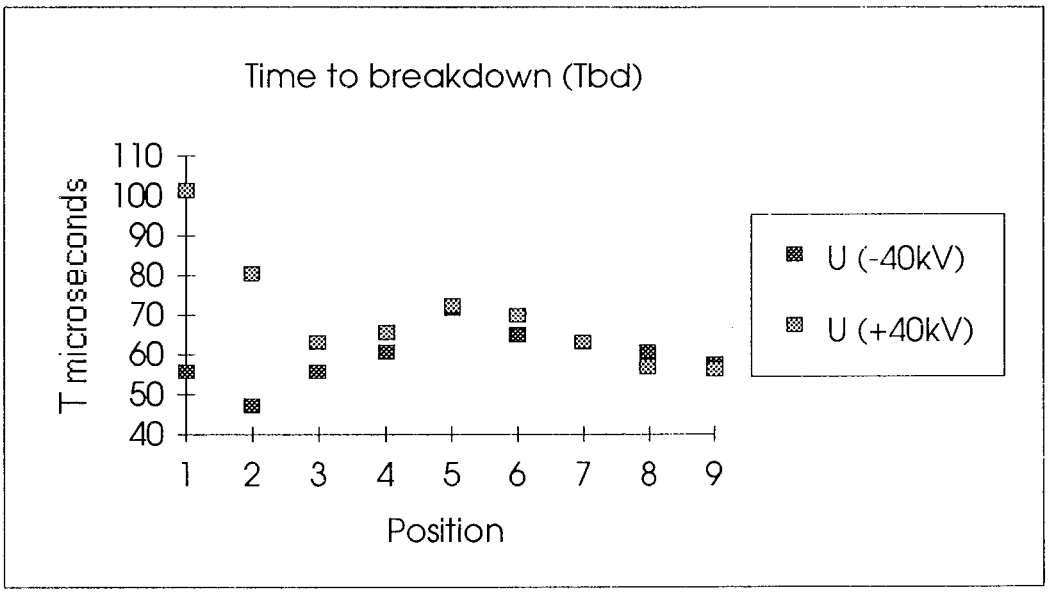

Fig [3.24] Tbd as a function of focal position.

The time to breakdown is larger in positive polarity than in negative, when the focal spot position is near the ground electrode. When the focal spot position is placed in the middle or towards the high voltage electrode, polarity does not seem to influence, see fig [3.24].

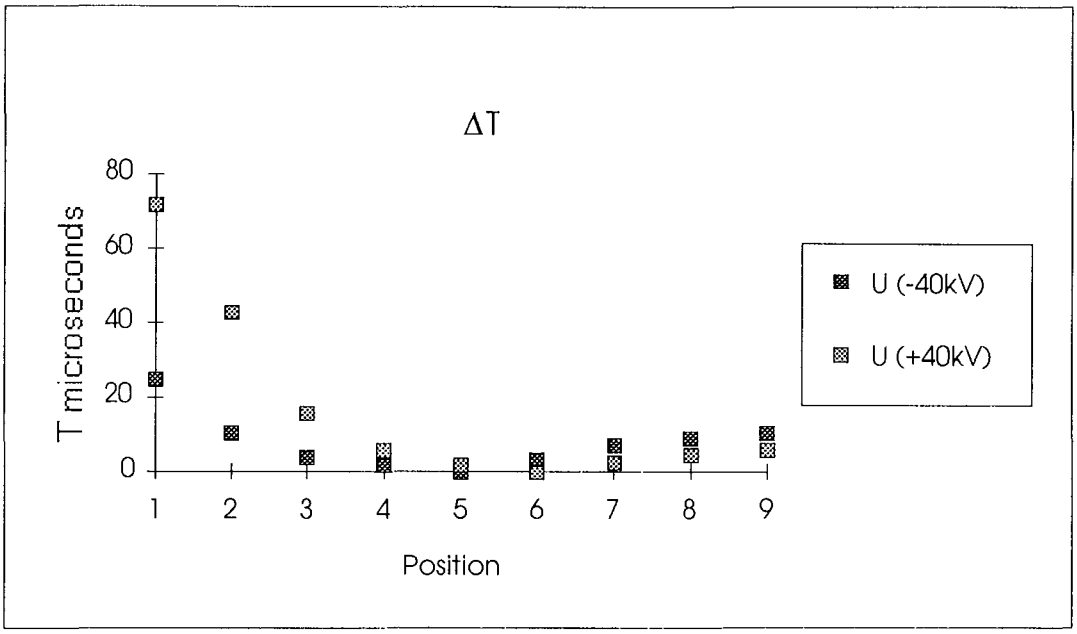

Fig [3.25] Time lag between large pulse and breakdown.

The time lag ΔT between the large pulse and the breakdown is largest when the focal spot is placed near the ground electrode. This is true in both polarities, but is more marked in positive polarity, see fig[3.25]. ΔT reaches a minimum when the focal spot is centered.

3.7 Fibre position

The last experiment performed was to investigate whether the position of the light collecting optical fibre had any influence on the results. The top angle of the light cone that a fibre possibly can see is determined by the numerical aperture, NA, and the refractive index of the liquid. A rough estimation of NA made it possible to calculate the angle α (20 °).

Choosing the correct distance y from the center line, between the electrodes made it possible to select a part of the gap that could be seen by the fibre. I chose a y so that 2x would be a third of the gap, see fig [3.26].

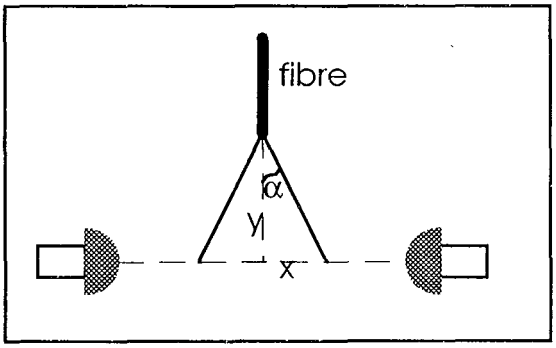

Fig [3.26] Fibre position, y=2.3 mm.

Before the measurements I thought that this arrangement would make it possible to see different light traces as the fibre was positioned at different locations, but that was not the case. The experiments showed that the light traces were similar as the fibre was moved across the gap. Probably was the photomultiplier over loaded (Later measurements have reported significant differences in light traces at different fibre positions !).

3.8 Correlation between light and current

The experiments were always conducted in such a way that both light and current were measured. By monitoring the two traces side by side, it was very easy to check the correlation. Correcting for transit time and pulse broadening in the photomultiplier, see appendix [2], it is shown that the correlation is good, both before and after the large pulse, see fig[3.27...28] and figures above.

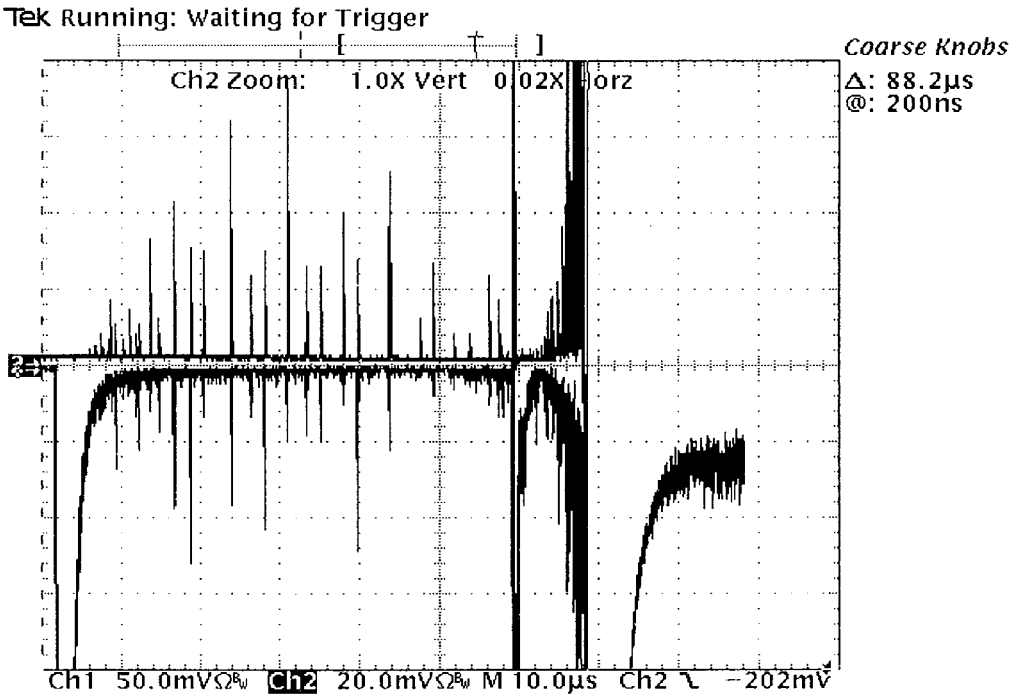

Fig [3.27] Light and current are correlated before the large pulse.
Applied voltage is +35 kV, Laser pulse energy is 100 mJ.
Upper trace is current and the lower is light.

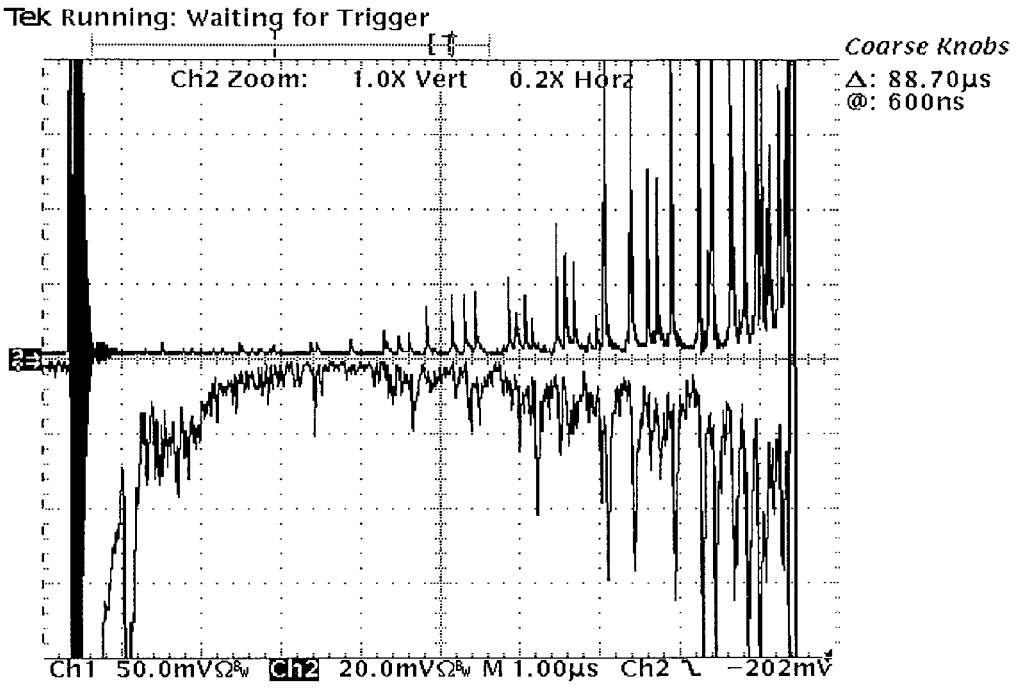

Fig [3.28] Light and current are correlated after the large pulse.
Applied voltage is +35 kV, laser pulse energy is 100 mJ.
Upper trace is current, lower is light.

3.9 Calibration

3.9.1 Calibration of current

To calibrate the current measurements I used a pulse generator. The pulse generator delivered a voltage pulse of variable length and height. To create a current pulse, a resistor (50 ohm) was placed in series. The current pulse was directly lead to the electrode connected to ground, see fig [3.29].

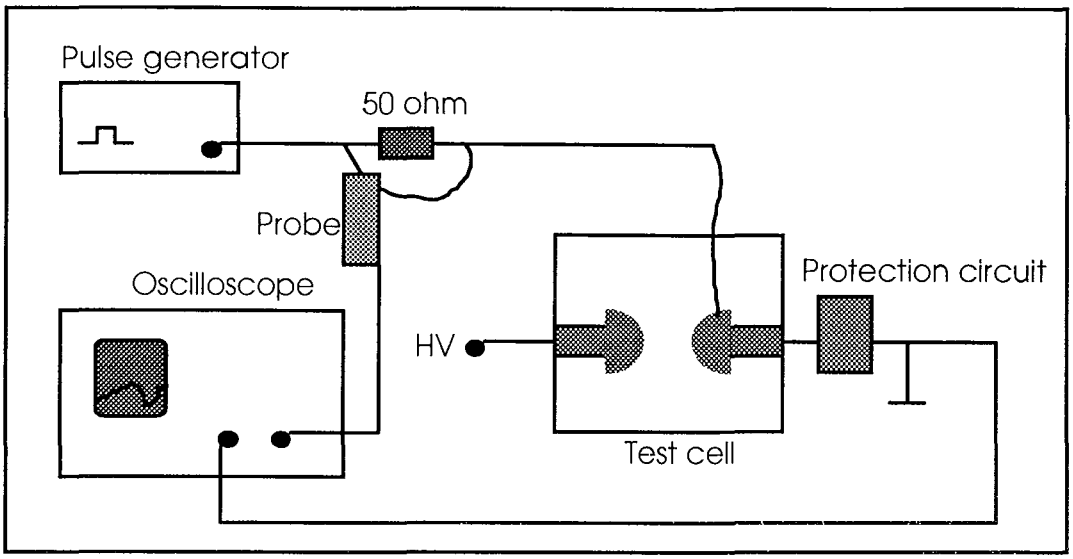

Fig [3.29] Current calibration set-up

The pulse that entered the system was measured with a high impedance probe. The two pulses were monitored on the oscilloscope where their amplitudes, rise times etc. could be compared. The length of the pulse (t_L) was chosen to be in the same order of magnitude as the current pulses measured in a prebreakdown process.

The result was calculated and the factor to be used for compensation is

$$i_{conv} = \frac{V_{in}}{V_{out}} \approx 2.75 \qquad [3.1]$$

The factor i_{conv} should always be used if a current measurement from an electrical breakdown has been done.

With help of an approximate formula (eq. [3.2]) it is possible to calculate the bandwidth (f_{BW}) of the in and output signal

$$f_{BW} = \frac{0.35}{t_r} \text{ [Hz]} \qquad [3.2]$$

where t_r is the rise time.

- Input: f_{BW}=42.94 [MHz] Output: f_{BW}=43.89 [MHz]

This result indicates that the protection circuit does not restrict the

bandwidth of the signal, at least up to 43 MHz.

3.9.2 Calibration of light

If the photomultiplier is used to detect a discrete spectrum of light, it is easy to calculate a relation between the anode current (output) and the number of photons (input) that hit the photo cathode. On the other hand, if the spectrum is continuous it is not that easy to find such a relation. The difficulty is due to the fact that photons with different wavelength produce a different amount of output signal. The result is that you can not, without knowledge about the spectral distribution of the emitted light, give an exact relation between input and output. However, previous measurements of the spectral components in a prebreakdown process, performed by P.Bårmann, LTH, has shown that the emitted light is continuous and can be approximated as constant. This simplification makes it possible to calculate a relation between the number of photons that hit the cathode and the output signal, but it will not be exact.

The set-up used for calibration is shown in fig [3.30].

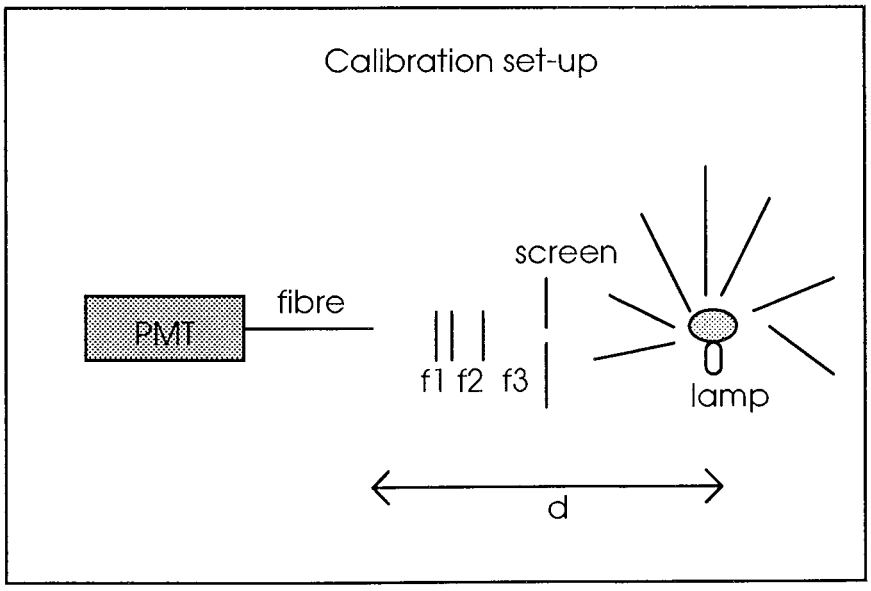

Fig [3.30] Light calibration set-up

The lamp was a calibration lamp from ORIEL and was held at constant distance (d) from the light collecting fibre. Its spectral irradiance $\phi_{e\lambda}(\lambda)$ was specified at different wavelengths (d=0.5m), see fig [3.31].

$$\phi_{e\lambda}(\lambda)\ [W/cm^2\ nm] \qquad [3.3]$$

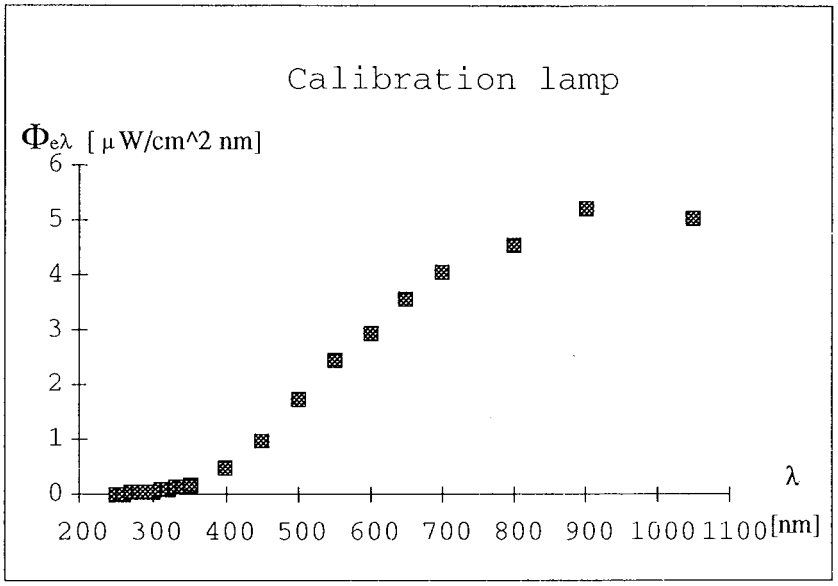

Fig [3.31] Spectral irradiance of the ORIEL lamp (d=0.5m).

Three filters, marked as f_1, f_2 and f_3 in fig [3.30], were used to restrict the light that finally reached the photomultiplier.

f_1 - This is an ordinary grey filter. It was manufactured by ORIEL and damped the light 10 times, i.e. the transmittance was 0.1. Let $f_1=0.1$.

f_2 - This filter was made by SCHOTT and was called NG10. Its transmittance depends on wavelength. Let $f_2 = f_2(\lambda)$.

f_3 - This is a cut-off filter. It works as an optical sliding door. A characteristic wavelength λ_c determines how open the door will be. Photons with wavelength λ will pass the filter if $\lambda > \lambda_c$ and will be blocked if $\lambda < \lambda_c$, see fig [3.32]. I used 13 different cut-off filters

and they all had different transmittances. They are denoted $f_3(\lambda)$.

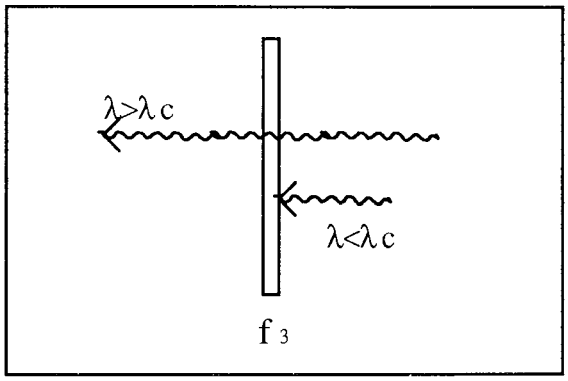

Fig [3.32] Cut-off filter with characteristic wavelength λ_c.

The lamp emits photons with wavelengths ranging from 250 to 2500 nm. The emitted power between the two wavelengths λ_1 and λ_2 is

$$\phi_e = \int_{\lambda_1}^{\lambda_2} \phi_{e\lambda}(\lambda) d\lambda \left[\frac{W}{cm^2}\right] \qquad [3.4]$$

Since the energy of a photon with wavelength λ_0 is

$$E(\lambda_0) = \frac{hc}{\lambda_0} \text{ [J]} \qquad [3.5]$$

It is possible to make a simple estimation of how many photons (n) that are emitted by the lamp between λ_1 and λ_2 per time and area, if λ_0 is chosen as

$$\lambda_0 = \frac{\lambda_1 + \lambda_2}{2} \text{ [nm]} \qquad [3.6]$$

The wavelength λ_0 then lies in the middle of the interval $[\lambda_1, \lambda_2]$. The number of emitted photons in the interval $[\lambda_1, \lambda_2]$ per time and area is then

$$n(\lambda_0) = \frac{\phi_e}{E(\lambda_0)} = \frac{\phi_e \lambda_0}{hc} \quad \left[\frac{\text{emitted photons } (\lambda_1 \rightarrow \lambda_2)}{\text{s cm}^2}\right] \qquad [3.7]$$

The three filters f_1, f_2 and f_3 reduce the number of photons that finally will reach the photomultiplier. Introduce $F(\lambda)$

$$F(\lambda) = f1 \cdot f2(\lambda) \cdot f3(\lambda) \qquad [3.8]$$

The number of photons in the interval λ_1 and λ_2 that reach the photomultiplier per unit time are $N(\lambda_0)$

$$N(\lambda_0) = A \cdot n(\lambda_0) \cdot F(\lambda_0) =$$
$$= A \cdot \frac{\Phi e \cdot \lambda 0}{h \cdot c} \cdot F(\lambda_0) \quad \left[\frac{\text{\# photons } (\lambda_1 \rightarrow \lambda_2)}{\text{s}}\right] \qquad [3.9]$$

where A is the fibre tip area

$$A = \pi \cdot r^2 \quad [\text{cm}^2] \qquad [3.10]$$

and λ_0 is calculated using equation [3.6]. The approximate value $N(\lambda_0)$ will be better as the interval $[\lambda_1, \lambda_2]$ gets smaller.

The use of cut-off filters makes it possible to calculate the contribution to the output signal from photons in a specified wavelength interval. Assume that two output signals Y_1 and Y_2 were recorded with the set-up in fig [3.30], and that two different cut-off filters with characteristic wavelengths λ_{c1} and λ_{c2} were used. From this it can be concluded that the signal Y_1 is the result of photons with wavelengths greater than λ_{c1}, the signal Y_2 results from photons with wavelengths greater than λ_{c2} and the difference Y

$$Y = Y_1 - Y_2 \qquad [3.11]$$

is thus the result of the photons in the wavelength interval $[\lambda_{c1}, \lambda_{c2}]$, see fig [3.33].

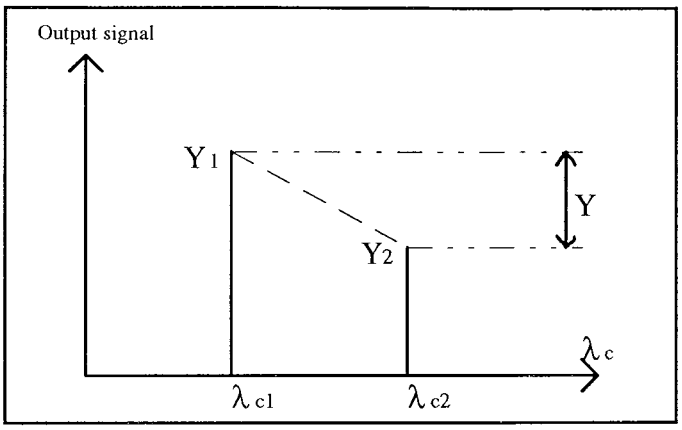

Fig [3.33] Two output signals

The 13 different cut-off filters I used each had their own characteristic wavelength.

$$\lambda cn \quad ,n = 1...13 \quad [\text{nm}] \qquad [3.12]$$

These wavelengths were ranging from 300 nm to 850 nm. This was a logical choice since the quantum efficiency of the photocathode of the photomultiplier is almost zero outside this interval, see appendix [2], which means that a photon with a wavelength outside this interval will not be registered by the PM-tube.

An output signal, Y_n n = 1...13, was measured with every filter, see fig [3.34].

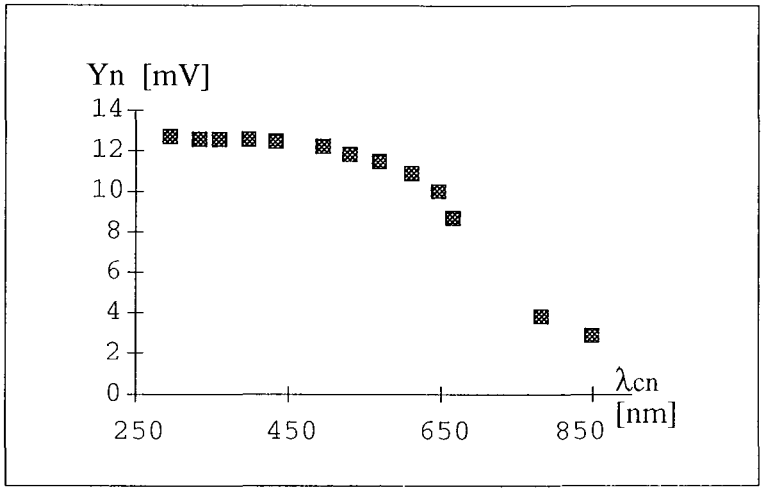

Fig [3.34] Recorded signal on the oscilloscope (Yn)
vs. characteristic wavelength (λcn) of the cut-off filter.

The contribution U_n to the output signal Y_n from the photons in the wavelength interval $[\lambda_{cn}, \lambda_{c(n+1)}]$ is then.

$$U_n = Y_n - Y_{n+1} \text{ [V]} \qquad [3.13]$$

Since a photomultiplier gives a current as output signal, let us convert U_n to a more convenient unit. Let

$$I_n = \frac{U_n}{R_{input}} = \frac{Y_n - Y_{n+1}}{R_{input}} \text{ [A]} \qquad [3.14]$$

where R_{input} = 50 Ω is the input impedance on the oscilloscope. I_n is plotted in fig [3.35].

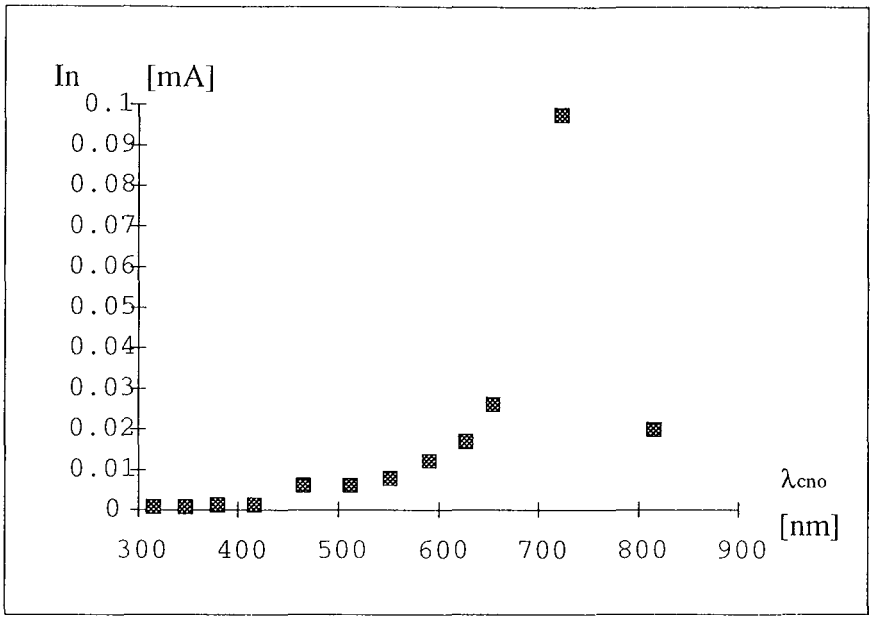

Fig [3.35] Differential anode current In.

Let us stop here for a moment and make a short summary.

- We know that the number of photons in the interval λ_{cn} to $\lambda_{c(n+1)}$ that reach the photomultiplier per unit time are $N(\lambda_{cn0})$, equation [3.9].

- We also know that the photons in the interval $[\lambda_{cn}, \lambda_{c(n+1)}]$ result in a contribution I_n to the total output signal I_{tot}.

It is thus possible to calculate the contribution to the output signal from each arrived photon in the interval $[\lambda_{cn}, \lambda_{c(n+1)}]$. Introduce i_n

$$i_n(\lambda_{cn0}) = \frac{I_n}{N(\lambda_{cn0})} = \frac{Y_n - Y_{n+1}}{R_{input} \cdot N(\lambda_{cn0})} =$$

$$= \frac{(Y_n - Y_{n+1}) \cdot h \cdot c}{R_{input} \cdot A \cdot F(\lambda_{cn0}) \cdot \Phi_e \cdot \lambda_{cn0}} \quad \left[\frac{\text{As}}{\text{arrived photon}}\right] \qquad [3.15]$$

where

$$\lambda_{cn0} = \frac{\lambda_{cn} + \lambda_{cn+1}}{2} \text{ [nm]} \qquad [3.16]$$

Assume now that the emitted light from the prebreakdown process consists of (λ_{C13} - λ_{C1}) number of photons* equally distributed over the spectrum, i.e. the photons have wavelengths ranging from λ_{C1} to λ_{C13} one photon per wavelength (nm). The output signal will then be

$$I_{tot} \approx \sum_{n=1}^{12} \left(i_n(\lambda_{nc0}) \cdot (\lambda_{c(n+1)} - \lambda_{cn}) \right) \left[\frac{\text{As}}{(\lambda_{c13} - \lambda_{c1}) \text{ \# of photons}} \right] \qquad [3.17]$$

I_{tot} has been calculated, see appendix [3], to be

$$I_{tot} = 1.859 \cdot 10^{-9} \left[\frac{As}{(\lambda_{c13} - \lambda_{c1}) \text{ photons}} \right] \qquad [3.18]$$

Which means that a current pulse with Δt seconds duration and a magnitude of I amperes (50 ohm input) will be the result of

$$\frac{I}{I_{tot}} \cdot \Delta t \cdot (\lambda_{c13} - \lambda_{c1}) \qquad [3.19]$$

number of photons.

---

* (λ_{C13} - λ_{C1}) = (850 - 295) = 555 number of photons

4 THEORY

This chapter is divided into three parts. In the first part (4.1) simple hydrodynamic models are used to investigate the long time lags recorded in the prebreakdown process. A possible model of the process will be presented. The second part (4.2) presents a short summary of electro magnetic radiation. In the last part (4.3) the calm period is examined. A simple model is used to explain the recorded current and light pulses.

4.1 Time lag

One possible explanation of the long delay in time between the triggering event and the electric breakdown is that a bubble filled with gas is formed. When the laser pulse hits the liquid a plasma is formed. The plasma burns hundreds of nanoseconds. When the plasma is extinguished a gas bubble is formed due to vaporisation. Initially the bubble is at high pressure which will cause the cavity to expand. Without any knowledge about the actual process I suggest four possible events that can take place.

Model 1 The bubble expands and collapses before it connects to any of the electrodes.

Model 2 The bubble expands and crosses the whole gap which results in a breakdown.

Model 3 The bubble expands and reaches one electrode.

Model 4 The expanding bubble is followed by a streamer that connects the gas bubble with one of the electrodes.

These four different models will be examined in order and I will try to show that it is the fourth model that is the most probable.

4.1.1 Model 1

The bubble does not reach any of the electrodes. Even if the formation, expansion and collapse of the bubble will act as perturbation of the system, which will enhance the breakdown probability, it does not explain the time lags recorded in the process. Therefore, this type of event will not be examined any further.

4.1.2 Model 2

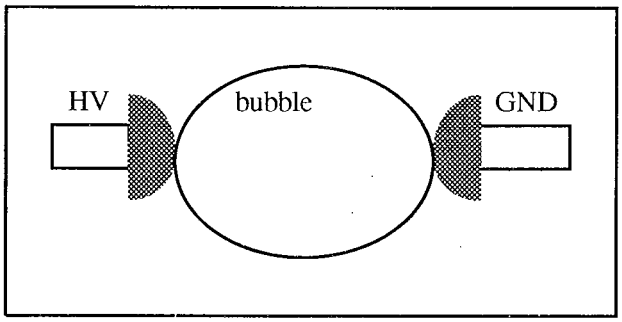

Fig [4.1] A cavity connects to both the electrodes.

The bubble expands and connects to both electrodes, see fig [4.1]. The electrode connection results in an electric breakdown. With help of Rayleigh theory it is possible to calculate the maximum radius of the expanded cavity [22], if one assumes a spherical growth. For an incompressible fluid we have

$$UR^2 = u(r)\cdot r^2 \quad \Rightarrow \quad u(r) = \frac{UR^2}{r^2} \qquad [4.1]$$

where R is the cavity radius and U=dR/dt. The kinetic energy (E) of the fluid surrounding the bubble is then

$$E = \frac{\rho}{2}\cdot\int_R^\infty u^2(r)\cdot 4\pi\cdot r^2\cdot dr = \frac{\rho}{2}\cdot\int_R^\infty \frac{U^2R^4}{r^4}\cdot 4\pi\cdot r^2\cdot dr =$$

$$= 2\pi\cdot\rho\cdot U^2\cdot\int_R^\infty \frac{R^4}{r^2}dr = 2\pi\cdot\rho\cdot U^2\left[-\frac{R^4}{r}\right]_{r=R}^{\infty} = 2\pi\cdot\rho\cdot U^2\cdot R^3$$

$$\because \quad E = 2\pi\rho U^2 R^3 \qquad [4.2]$$

where ρ is the fluid density. But as a bubble expands it does work against the external pressure P_a. Thus for a system with initial kinetic energy E_0 the energy balance equation can be written

$$E_0 = 2\pi\rho U^2 R^3 + \frac{4}{3}\pi R^3 \cdot P_a \qquad [4.3]$$

where the first term is the kinetic energy of the surrounding liquid and the last term is the work against the external pressure. Rearranging eq.[4.3] we get an expression relating velocity, radius and energy

$$E_0 = 2\pi\rho U^2 R^3 + \frac{4}{3}\pi R^3 \cdot P_a \quad \Rightarrow$$

$$\Rightarrow \quad U^2 = \frac{E_0}{2\pi\rho \cdot R^3} - \frac{2}{3}\cdot\frac{P_a}{\rho} \qquad [4.4]$$

When U=0 the cavity has reached its maximum radius R_m.

$$U = 0 \quad \Rightarrow \quad \frac{E_0}{2\pi\rho \cdot R^3} = \frac{2}{3}\cdot\frac{P_a}{\rho}$$

$$\Rightarrow \quad R_m^3 = \frac{3}{4\pi}\cdot\frac{E_0}{P_a} \qquad [4.5]$$

Assume now that about 10% of the measured energy of the laser pulse is transferred into kinetic energy. The rest is used for vaporisation or is lost due to absorption. If the ambient pressure is one atmosphere we have

$$R^3{}_m = \frac{3}{4\pi}\cdot\frac{0.10 \cdot E \cdot 10^{-3}}{10^5} \ [\mathrm{m}^3] \qquad [4.6]$$

$$\Rightarrow \quad Rm = 6.204 \cdot 10^{-4} \cdot \sqrt[3]{E} \ [\mathrm{m}] \qquad [4.7]$$

where E [mJ] is the measured energy outside the test cell. As shown in fig [4.2] the maximum radius is as big as half the gap length when the

laser pulse energy is 65 [mJ].

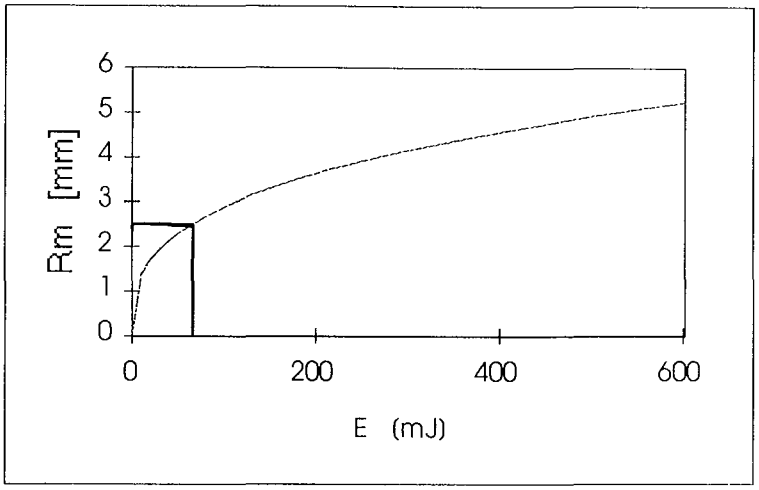

Fig [4.2] Maximum radius versus input energy.

However, even if it is possible to expand the cavity far enough it does not explain the recorded time lags, see fig [3.23].

The expansion of the vapor bubble stops when the kinetic energy of the system passes through zero. At this point the cavity is fully expanded and the internal pressure is far below the ambient which causes the bubble to collapse. The work done by the external pressure [22] is then

$$W_a = \frac{4\pi}{3} \cdot P_a \cdot \left(R_m^3 - R^3\right) \quad [\mathrm{J}] \qquad [4.8]$$

The work W_a should equal the kinetic energy of the surrounding liquid, eq. [4.2]

$$W_a = \frac{4\pi}{3} \cdot P_a \cdot \left(R_m^3 - R^3\right) = 2\pi\rho \cdot U^2 \cdot R^3 \qquad [4.9]$$

which gives

$$U^2 \cdot R^3 = \frac{2}{3} \cdot \frac{P_a}{\rho} \cdot \left(R_m^3 - R^3\right) \quad \Rightarrow$$

$$\Rightarrow \quad U(R) = \sqrt{\frac{2}{3} \cdot \frac{P_a}{\rho}} \cdot \sqrt{\frac{R_m^3 - R^3}{R^3}} \qquad [4.10]$$

Integrating equation [4.10] gives the time it will take for the bubble to collapse

$$\tau = \int_0^{R_m} \frac{dR}{U(R)} \quad [\mathrm{s}] \qquad [4.11]$$

which has been calculated to be, see [22]

$$\tau = R_m \sqrt{\frac{\rho}{6P_a}} \frac{\Gamma\left(5/6\right) \cdot \Gamma\left(1/2\right)}{\Gamma\left(4/3\right)} = 0.915 \cdot R_m \cdot \sqrt{\frac{\rho}{P_a}} \qquad [4.12]$$

where $\Gamma(n)$ is the gamma function. By symmetry τ is also the time for bubble expansion, which means that the expansion time can be expressed, using equation [4.7], as

$$\tau_{exp} = 6.204 \cdot 10^{-4} \cdot \sqrt[3]{E} \cdot 0.915 \cdot \sqrt{\frac{\rho}{P_a}} \quad [\mathrm{s}] \qquad [4.13]$$

where E is the energy of the laser pulse [mJ], measured outside the test cell.

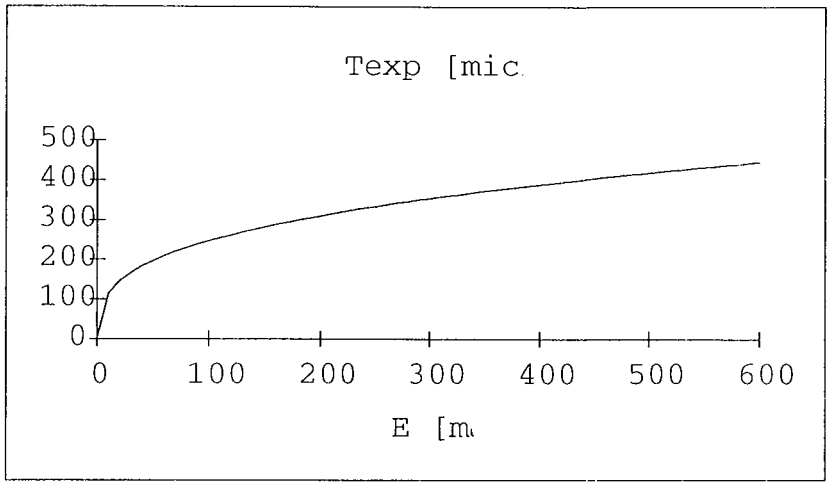

Fig.[4.3] Expansion time (τ_{exp}) versus measured energy.

As can be seen in fig [4.3], the expansion time for a 5 mm cavity (E=65 mJ), is much longer than the time lag recorded in the experiments with different laser pulse energies, see section [3.5]. This type of event does not support the collected data so let us look at next model.

4.1.3 Model 3

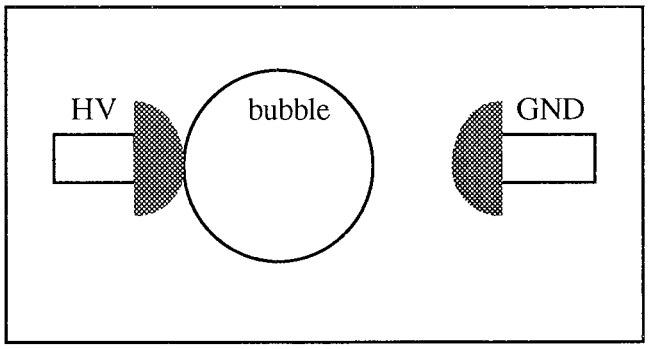

Fig [4.4] The bubble connects to one of the electrodes.

The bubble expands and reaches one electrode, see fig[4.4]. This can be due to two facts. First, the origin of the cavity, i.e. the focal spot of the laser light, is close to one electrode. Therefore the bubble will reach this electrode as it expands before it reaches the other. Second, the bubble is affected by an electrostatic force which will make it elongate against one electrode.

The second explanation can be ruled out if we look at the bubble as a plasma which will be quasi neutral. The first explanation however, is possible. The large pulse that can be observed in the current traces, can then be explained as the moment when the cavity connects to one of the electrodes. At the same instant the bubble reaches the electrode it will become equipotential, which implies that a gas discharge immediately takes place. The cavity connection results in a sudden change in gap length. If the radius of the cavity is R when it connects to the electrode, the gap length will reduce from L to L-2R. This reduction in gap length will enhance the breakdown probability.

Let us consider this process more in detail. Assume that the pulse energy is 165 mJ, which results in a maximum radius of about R_m=3.4 mm, see equation [4.7]. Further, assume that the focal position is located at a distance D from one of the electrodes, see fig [4.5]. Observe now, if D>R_m (or (L-D)>R_m) the process is not possible.

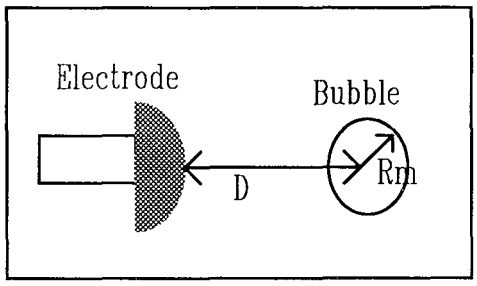

Fig [4.5] Bubble outside electrode.

In the beginning of the cavity expansion the work against the ambient pressure can be ignored. In equation [4.2] we have calculated the kinetic energy of the surrounding fluid to be

$$E = 2\pi\rho U^2 R^3 \qquad [4.2]$$

where R is the bubble radius, U=dR/dt and ρ is the fluid density. If the kinetic energy of the system is constant, E=E_0, we have

$$U^2 = \left(\frac{dR}{dt}\right)^2 = \frac{E_0}{2\pi\rho \cdot R^3} \quad \Rightarrow$$

$$\Rightarrow \quad \frac{dR}{dt} = \sqrt{\frac{E_0}{2\pi\rho}} \cdot \frac{1}{\sqrt{R^3}} \quad \Rightarrow$$

$$\Rightarrow \quad \sqrt{R^3}\,dR = \sqrt{\frac{E_0}{2\pi\rho}}\,dt \quad \Rightarrow$$

$$\Rightarrow \quad \int \sqrt{R^3}\,dR = \frac{2}{5} \cdot \sqrt{R^5} = \sqrt{\frac{E_0}{2\pi\rho}} \cdot \int dt = \sqrt{\frac{E_0}{2\pi\rho}} \cdot t + R_0'$$

$$\Rightarrow \quad R(t) = \left[\frac{5}{2}\sqrt{\frac{E_0}{2\pi\rho}} \cdot t\right]^{2/5} + R_0 \approx \left(\frac{E_0}{\rho}\right)^{1/5} \cdot t^{2/5}$$

$$\because \qquad R(t) \approx \left(\frac{E_0}{\rho}\right)^{0.2} \cdot t^{0.4} \quad [\text{m}] \qquad [4.14]$$

The equation [4.14] has been plotted in fig [4.6]. In chapter 3, see section [3.6], the time to the large pulse was measured as a function of focal position, see fig [3.23].

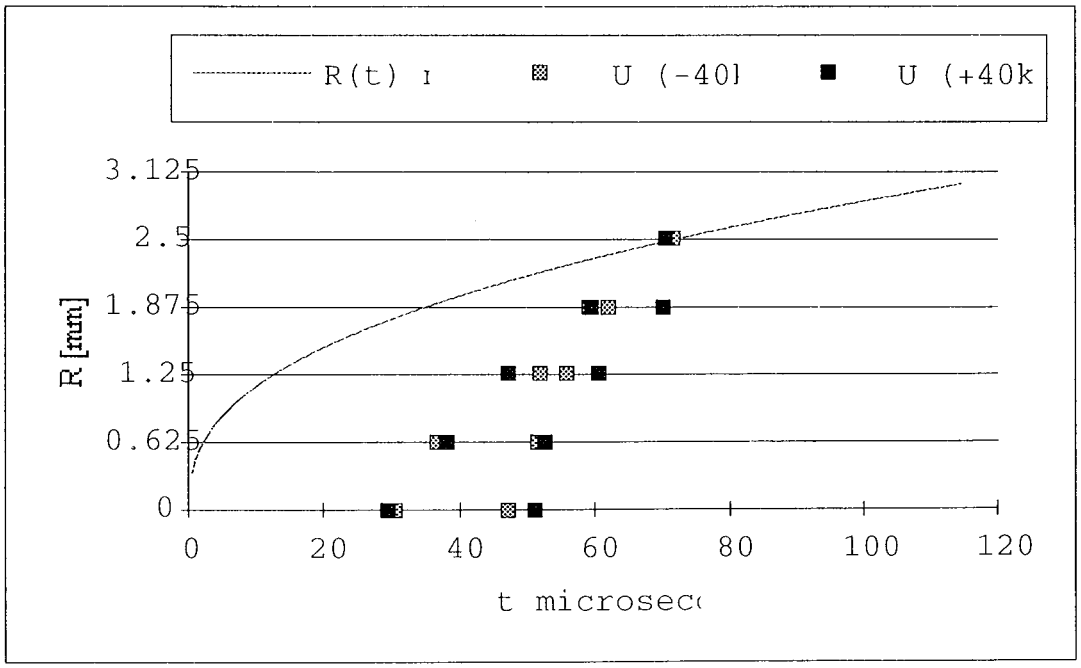

Fig [4.6] Plot of bubble radius versus time, using equation [4.14].
Data from fig [3.23] also have been included.

If the large pulse was the result of the connection between the cavity and one of the electrodes the plot R(t), eq. [4.14], should coincide with the measured time lags presented in fig [3.23]. I have combined the data from fig [3.23] and the plot of R(t), see fig [4.6], and it can be seen that the curves do not match. Therefore, it appears that this explanation is not correct.

4.1.3 Model 4

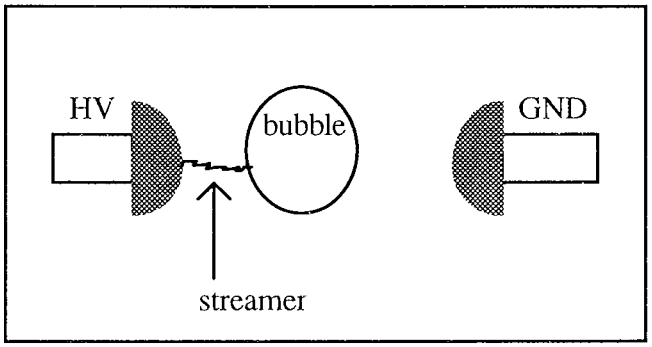

Fig [4.7] A streamer connection.

The expanding bubble is followed by a streamer that connects the gas bubble with one of the electrodes. The large pulse is then caused by the connecting streamer.

One way to view such a process is to assume that the bubble expands until it reaches a critical state when a rapidly growing instability of the surface of the cavity leads to a vapor streamer [20]. The streamer bridges the gap to the closest electrode. The streamer connection results in the bubble becoming equipotential.

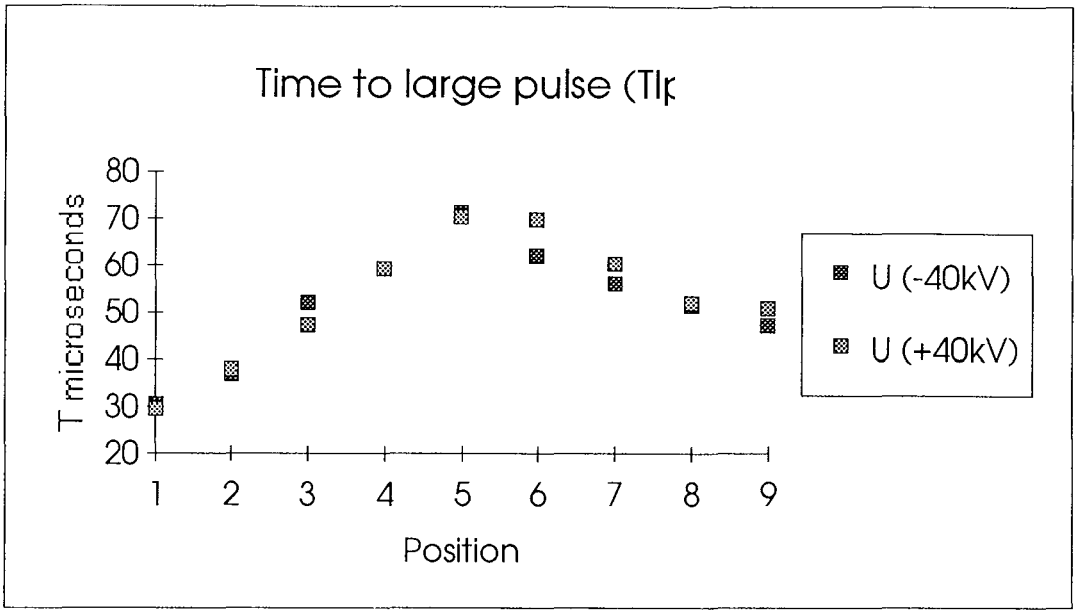

Fig [3.23] Tlp as a function of position.

Let us stop here for a second. As can be seen in fig [3.23], the time to the large pulse has a maximum when the focal spot is placed in the middle of the gap (pos 5). This can be understood as when the bubble has reached its critical state, the distance between the cavity wall and the electrode is the greatest. (This is true if the size of the bubble, when it is in a critical state, does not depend on focal position.) Taking one step towards the ground electrode (pos 4) one can see that the time to the large pulse is less than if going towards the high voltage electrode (pos 6). This assymetry might be due to that the connecting streamers have different polarities. The time difference (ΔT) between the time to the large in position 4 and position 6 is then the result of streamers with different propagation speeds make the connection between the electrodes and the bubbles centered in position 4 and 6. A faster streamer connects the electrode with the bubble in position 4. In the literature concerning prebreakdown phenomena one often finds that the positive streamer is one order of magnitude faster than the negative [14].

If the radius of the bubble is R when the streamer starts propagating, the distance (X(pos)) to the closest electrode is

$$X(pos)=L/2-FP-R \qquad [4.15]$$

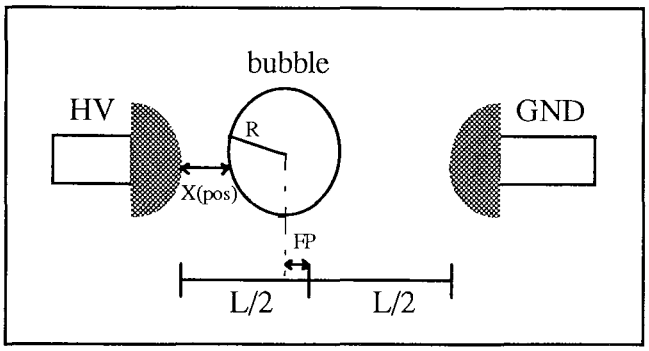

Fig [4.8] Illustration of equation [4.15].

where 'pos' is the focal position (1..9) and FP is the distance between the middle of the gap and 'pos', see fig [4.8]. Thus X(4)=X(6). Assume now that the positive streamer has a constant velocity of about v_+=2 [km/s], which gives a propagation time of

$$T_{p+} = \frac{X(4)}{v_+} \approx 1\mu s \qquad [4.16]$$

The propagation time for the negative streamer is then

$$T_{p-} = \frac{X(6)}{v_-} = \frac{X(4)}{v_+/10} = 10 \cdot T_{p+} \approx 10\mu s \qquad [4.17]$$

if $v_-=v_+/10$. The time difference T should then be in the region of 9 microseconds which can be observed in fig [3.23]. This looks promising so far.

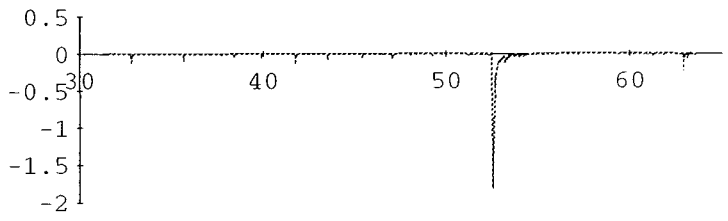

Fig [4.9] Light trace. Large pulse at 52.6 μs.
Position 3, applied voltage +40 kV, laser pulse energy 165 mJ.
The large pulse is preceded by a positive streamer.

When the connection between the electrode and the cavity is made the bubble has the same potential as the connected electrode.

Closest electrode from focal spot	Polarity of Applied high voltage	Connecting streamer	Cavity after connection	Potential of Cavity after connection
+HV	+	-	+	+HV (pos 6...9)
GND	+	+	-	GND (pos 1...4)
-HV	-	-	-	-HV (pos 6...9)
GND	-	+	+	GND (pos 1...4)

Tab [4.1]

When the applied high voltage is +HV and the bubble has a positive polarity (pos 6...9) it seems like a positive streamer emanates from the cavity towards the ground electrode which explains the short time intervals between the large pulse and the breakdown, see fig [3.25] and fig [4.10].

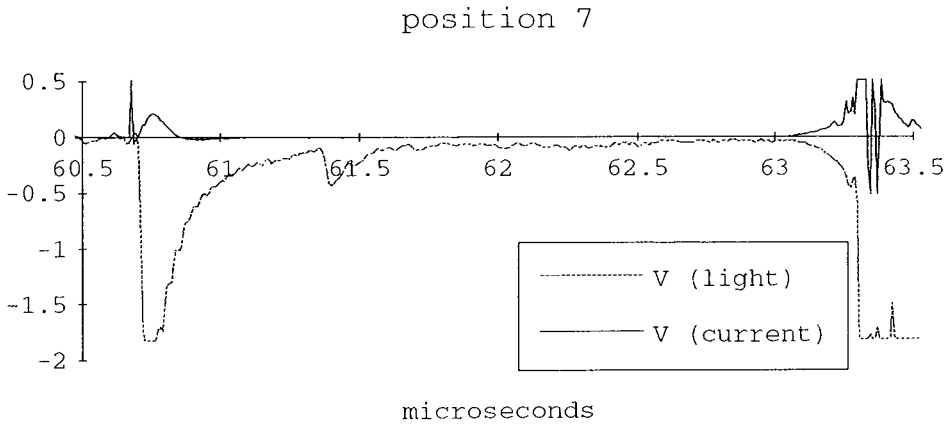

Fig [4.10] Applied voltage +40 kV, laser pulse energy 165 mJ
Positive streamer precedes breakdown (63.4 μs).

In the case the bubble has a zero potential and applied voltage is +HV,

there is a long delay between large pulse and breakdown, see fig [3.25] (pos 1...4). Current recordings during this phase, see fig [4.11...4.12], suggest that the phase ends with a negative connecting streamer since a lot of fast current pulses can be found, which is a characteristic feature.

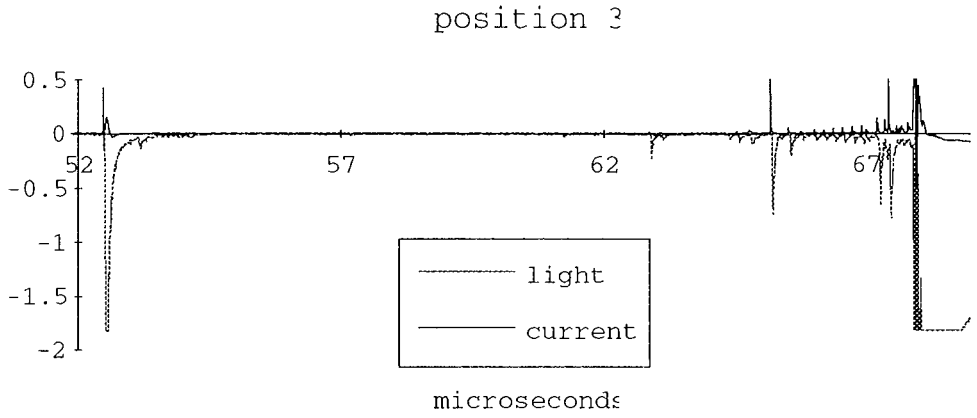

Fig [4.11] Applied voltage +40 kV, laser pulse energy 165 mJ.
Breakdown (68.2 μs) precedes by a negative streamer.

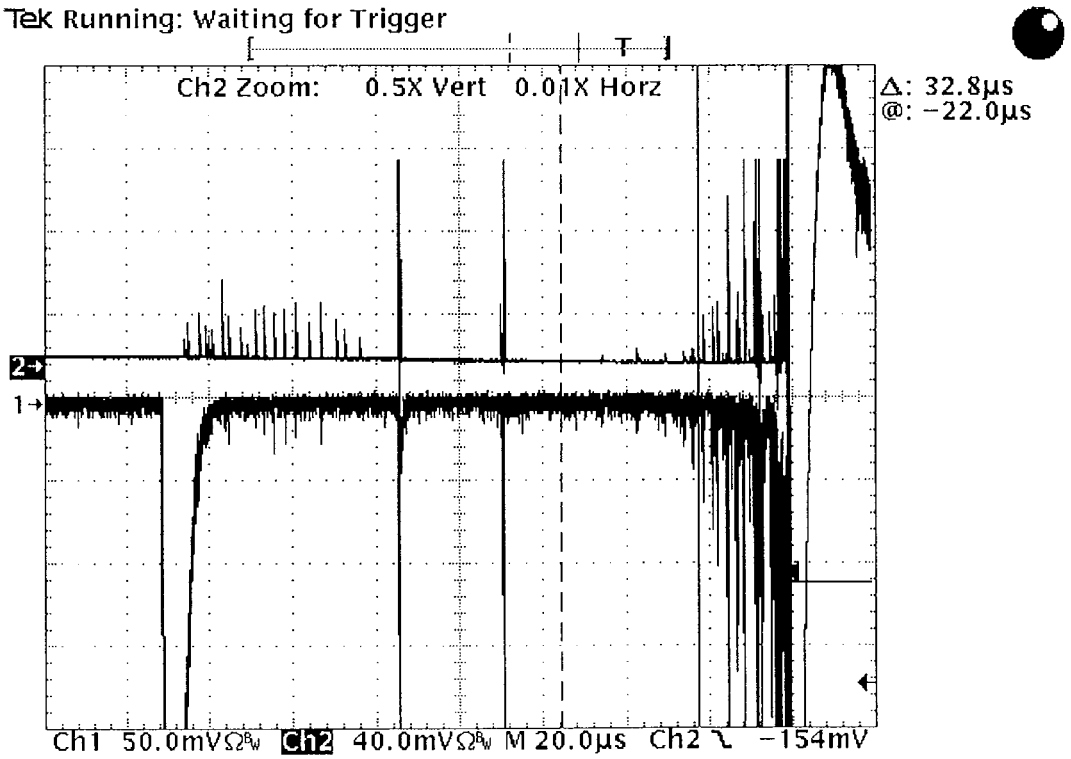

Fig [4.12] Position 2, applied voltage +35 kV, laser pulse energy 100 mJ.

When the applied high voltage is -HV and the focal position is closer to the high voltage electrode (-HV), the connected bubble receives a negative polarity. Current traces, see fig [4.13], reveals fast current pulses which suggests that a negative streamer emanates from the cavity and propagates towards the ground.

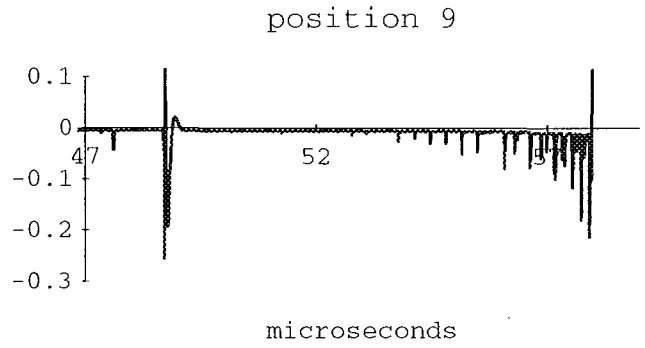

Fig [4.13] Applied voltage -40 kV, laser pulse energy 165 mJ.
Breakdown (58 μs) precedes by a negative streamer.
Current trace.

If the focal spot is closer to the ground electrode, symmetry would result in a positive emanating streamer, but in fig [3.25] one can see that there is a long delay in time between breakdown and large pulse (pos 1..4). Current recordings do not show any fast current pulses, instead a calm period can be seen that ends in a sudden breakdown, see fig [4.14]. One possible explanation is that the bubble continues growing, which explains the long time lag, until a second instability at the surface of the cavity results in an emanating positive streamer.

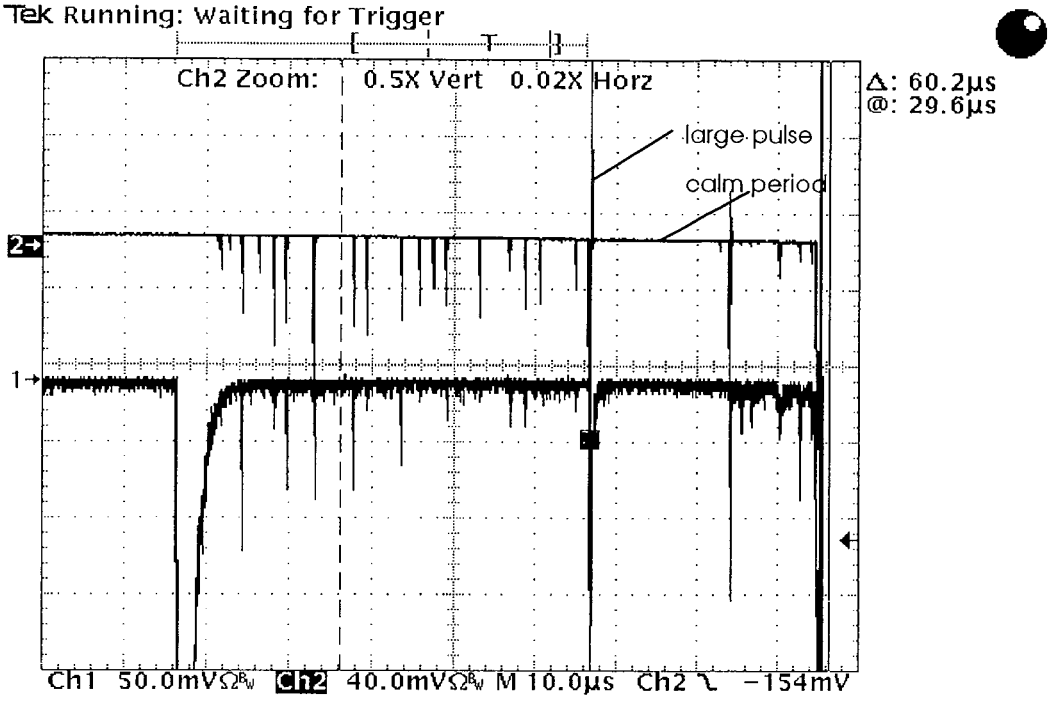

Fig [4.14] Position 2, applied voltage -35 kV, laser pulse energy 100 mJ

Let us look at the connecting streamers more schematically. If we denote the first streamer with (1) and the second with (2) we can make a schematic plot of the process, see fig [4.15].

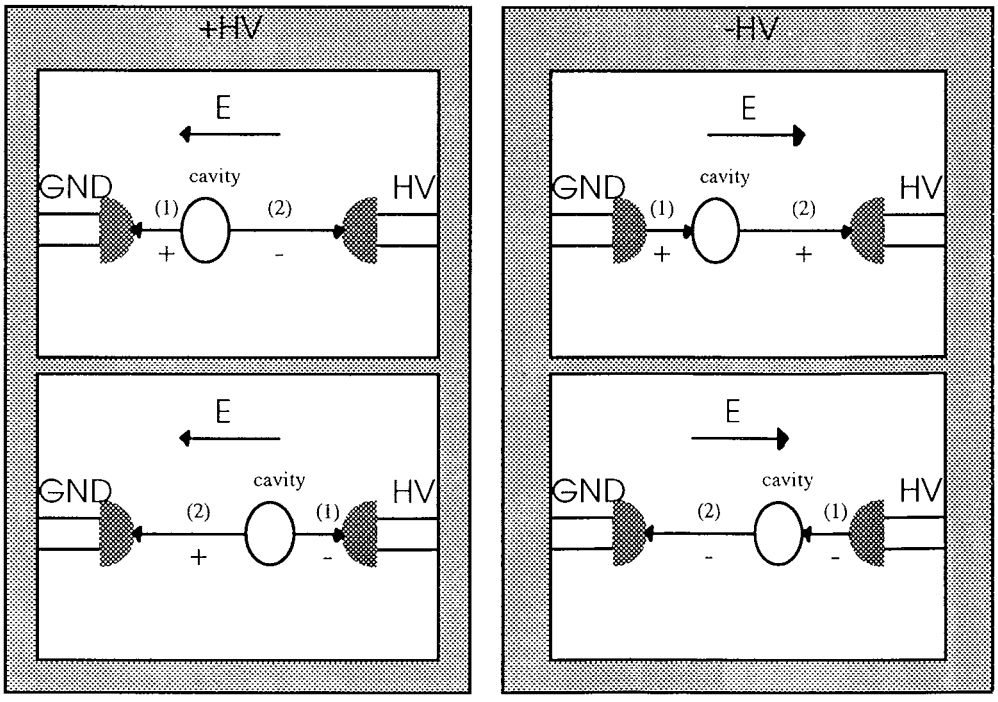

Fig [4.15] Different streamer connections.
The numbers 1 and 2 indicate in which order
the streamers start propagating, + and - denotes
the polarity of the streamer.

As can be seen in fig [4.15] there is one major difference between the processes, when the applied high voltage is positive both streamers emanate from the cavity while in the negative case only the second streamer starts propagating from the bubble. This difference might be the reason why the time lags recorded in the process do not show the expected antisymmetry, look at fig [3.23] for example. Maybe the appropriate way to treat the prebreakdown process is to distinguish between positive and negative (+HV and -HV) prebreakdown process.

When the whole gap is bridged, the electric breakdown is a fact.

4.1.5 Summary

The laser triggered breakdown process constitutes of five main events.

1 **The trigger mechanism** - Energy is transferred into the system by a focused laser pulse, see fig [4.16]. A plasma is formed.

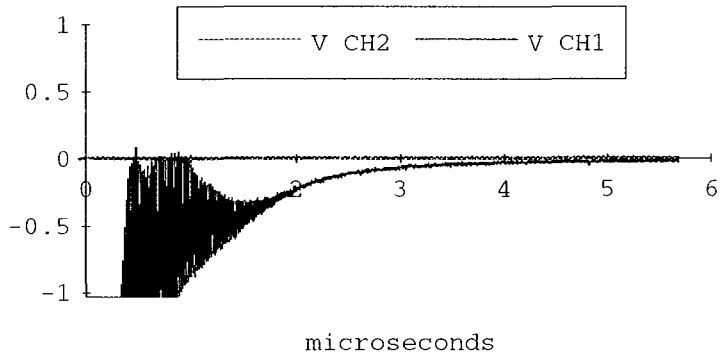

Fig [4.16] Applied voltage +40 kV, laser pulse energy 100 mJ, position 5.
The laser pulse hits the liquid at T = 0 μs.
CH2 is current and CH1 is light.

2 **The bubble** - A gas filled cavity is formed and it expands due to

high pressure. Discharges occur inside the bubble, see fig [4.17].

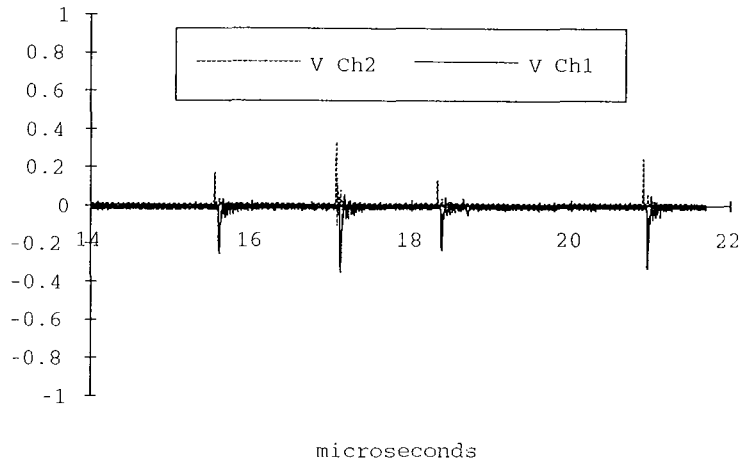

Fig [4.17] Applied voltage +40 kV, laser pulse energy 100 mJ, position 5.
Light and current are well correlated.
CH2 is current and CH1 is light.

3 First streamer - An instability of the surface of the bubble develops into a streamer that connects to one of the electrodes, see fig [4.18].

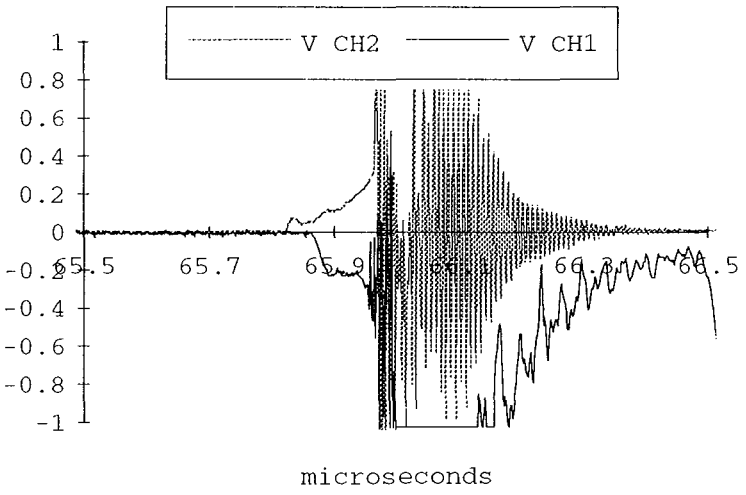

Fig [4.18] Applied voltage +40 kV, laser pulse energy 100 mJ, position 5.
The large pulse (65.95 μs) is preceded by a positive streamer.
CH2 is current and CH1 is light.

4 Second streamer - The streamer bridges the remaining gap, see fig

[4.19].

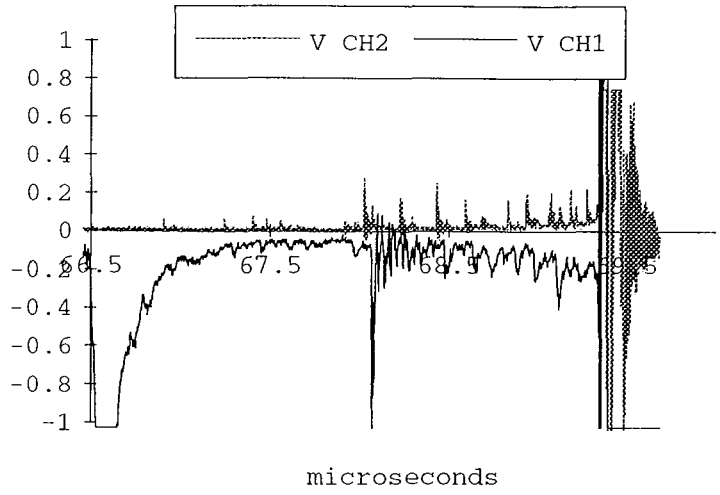

Fig [4.19] Applied voltage +40 kV, laser pulse energy 100 mJ, position 5.
The second streamer (negative) bridges the rest of the gap,
which results in a breakdown (69.5 μs).
CH2 is current and CH1 is light.

5 **Breakdown** - The connection of the two electrodes immediately results in a breakdown.

4.2 Radiation

When electric charges are accelerated or decelerated they produce electromagnetic radiation. Charges existing in an electric field will be affected by the Lorentz force

$$F_{Lorentz} = q \cdot E = m_Q \cdot a \qquad [4.18]$$

which will produce an acceleration (a). In the case where we have two electrodes at different potentials, producing an electric field, every charge created will be accelerated and therefore radiate. The radiation (γ) is thus related to

$$\gamma \propto \frac{\partial^2 x}{\partial t^2} \qquad [4.19]$$

There are other sorts of radiation but they will not be considered here. In a partial discharge inside a cavity, a distinct number of charge carriers is released. The number released is proportional to the stored energy in the local region. The charge carriers are accelerated by the electric field inside the cavity which make them radiate.

The current is measured as the rate of change of charges, induced by moving charges in the electrode gap, on one of the electrodes. It is not measured as the arrived number of charges per unit time. The current (I) is thus related to the velocity of the charges in the gap.

$$I \propto \frac{\partial x}{\partial t} \qquad [4.20]$$

These relations make it possible to say something about how well correlated the current and the light should be. Fig [4.20] (upper trace) shows a typical current trace. If we assume that the radiation is only caused by accelerated charges (a simplification) the light and current should be correlated in time. The light trace (lower trace) in fig [4.20] verifies the assumption.

4.3 The calm period

Earlier in this work I have described the time interval between the initiating event and the breakdown as calm and in the previous section it was explained as bubble expansion. During this expansion, distinct pulses can be seen in the current and light recordings, see fig [4.20]. The pulses are assumed to be discharges in the cavity.

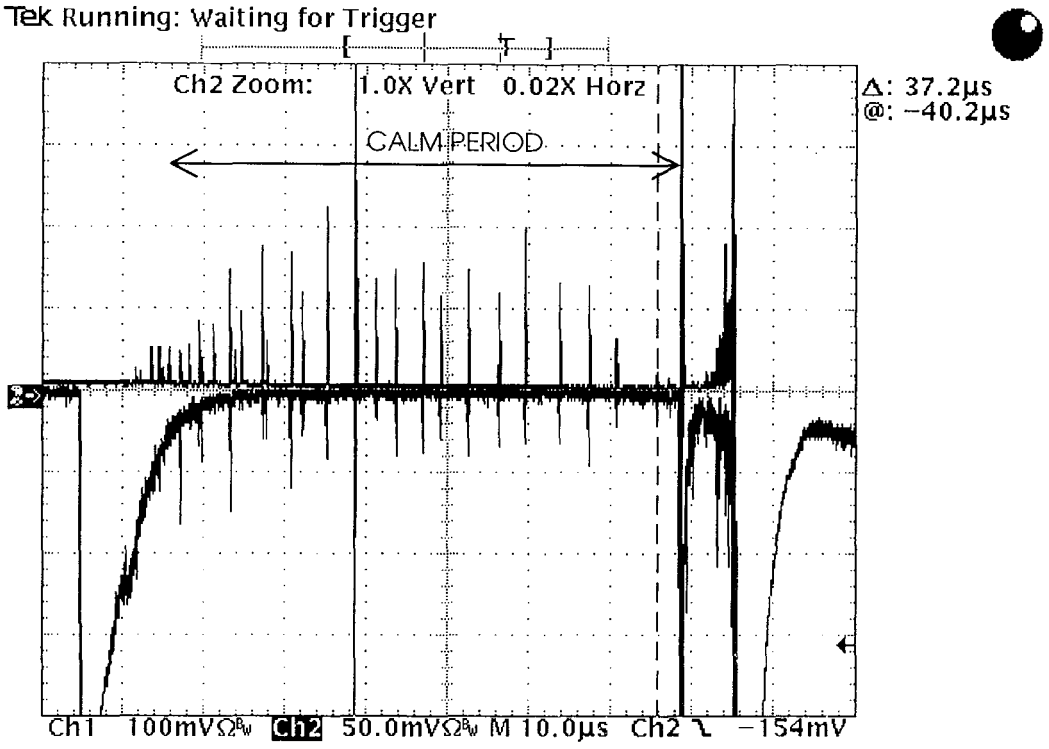

Fig [4.20] Distinct pulses in the calm period.
Applied voltage is +35 kV, laser pulse energy is 150 mJ

One way to describe the current measurements is to look at the test cell as a capacitor. A change in current is then a result of a change in capacitance between the two electrodes. Assume that the system can be modelled by the following configuration, [23], see fig [4.21].

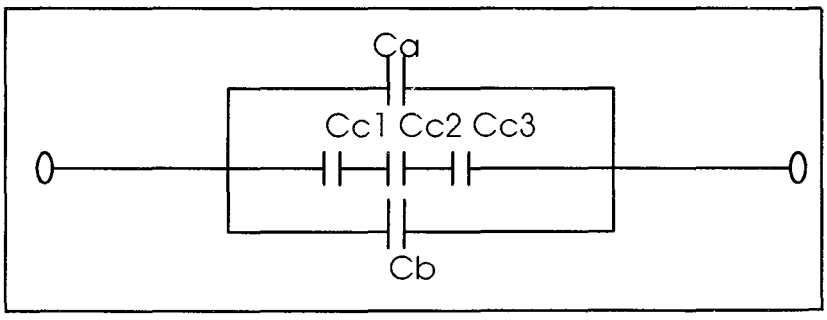

Fig [4.21] Model of the test cell.

The total capacitance between the electrodes is then

$$C = C_a + C_b + C_c \qquad [4.21]$$

where

$$\frac{1}{C_c} = \frac{1}{C_{c1}} + \frac{1}{C_{c2}} + \frac{1}{C_{c3}} \qquad [4.22]$$

If a gas filled bubble is generated in the middle of the gap, see fig [4.22],

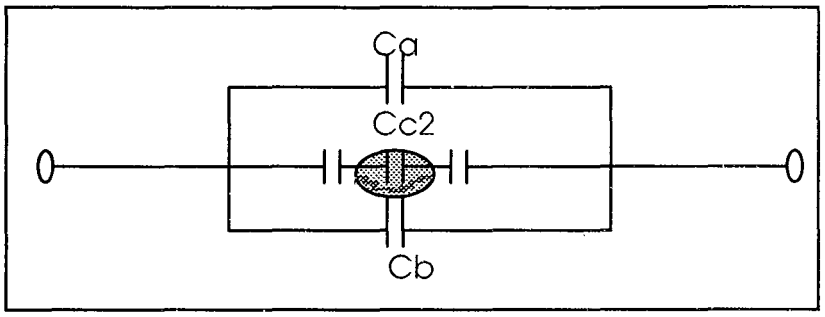

Fig [4.22] A gas filled cavity in the test cell.

the capacitor C_{c2} will be disconnected if a discharge occurs. The discharge has a short duration in time (ns range) and will therefore only alter the total capacitance C for a short time. During this time C will be

$$C = C' = C_a + C_b + C'_c \qquad [4.23]$$

where

$$\frac{1}{C'_c} = \frac{1}{C_{c1}} + \frac{1}{C_{c3}} \qquad [4.24]$$

The change in capacitance results in a current pulse, through

$$I(t) = \frac{dQ}{dt} = U \cdot \frac{dC}{dt} \qquad [4.25]$$

where U is the voltage applied to the test cell. In an AC voltage field these discharges will be repetitive due to the rise and fall of the applied voltage. However, in a DC voltage field, as in my case, the discharge will neutralise the electric field inside the cavity so there would just be one single discharge. Therefore, in order to explain the many pulses recorded, we have to look for other reasons why the total capacitance C could change. There are two possibilities, proposed by S. Kröll, to change the capacitance:

1 **Bubble radius (r)** - If the bubble changes its radius the change in capacitance will be

$$\frac{\partial C}{\partial t} = \frac{\partial C}{\partial r} \cdot \frac{\partial r}{\partial t} \approx \frac{\partial C}{\partial r} \cdot \frac{\Delta r}{\Delta t} \qquad [4.26]$$

2 **Dielectric constant (ε)** - If the relative dielectric constant ε_r changes its value, the change in capacitance is

$$\frac{\partial C}{\partial t} = \frac{\partial C}{\partial \varepsilon_r} \cdot \frac{\partial \varepsilon_r}{\partial t} \approx \frac{\partial C}{\partial \varepsilon_r} \cdot \frac{\Delta \varepsilon_r}{\Delta t} \qquad [4.27]$$

That the value $\Delta\varepsilon_r/\Delta t$ differs from zero is not that obvious, but it can be thought of as a quantity to model the number of charge carriers present in the liquid. The total derivative will then be

$$\frac{dC}{dt} = \frac{\partial C}{\partial r} \cdot \frac{dr}{dt} + \frac{\partial C}{\partial \varepsilon_r} \cdot \frac{d\varepsilon_r}{dt} \qquad [4.28]$$

which gives

$$I(t) = U \cdot \left(\frac{\partial C}{\partial r} \cdot \frac{dr}{dt} + \frac{\partial C}{\partial \varepsilon_r} \cdot \frac{d\varepsilon_r}{dt} \right) \qquad [4.29]$$

Assume now that the radius of the bubble is r = a. The configuration then looks like this, see fig [4.23].

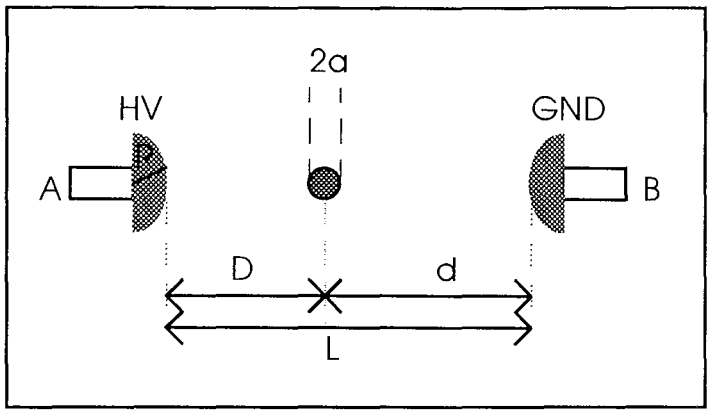

Fig [4.23] Bubble between electrodes.

The equivalent circuit becomes

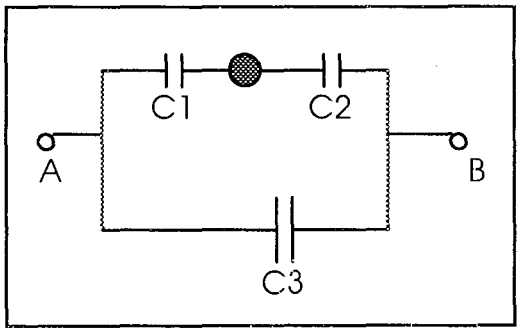

Fig [4.24] Equivalent circuit.

The total capacitance between the electrodes A and B is then

$$C = \frac{C_1 \cdot C_2}{C_1 + C_2} + C_3 \qquad [4.30]$$

In order to simplify the calculations, assume that the radius of the hemispherical electrodes is much bigger than the bubble radius. The electrodes can then be approximated by planes with area S. We then have

$$C_3 = \varepsilon_0 \varepsilon_r \cdot \frac{S}{L} \qquad [4.31]$$

The capacitance between a sphere and a plane can be calculated with the

method of images, see appendix [4]. The capacitors C_1 and C_2 are then

$$\begin{aligned} C_1 &= 4\pi\varepsilon_0\varepsilon_r \cdot a \cdot \left(1+\alpha+\frac{\alpha^2}{1-\alpha^2}+\ldots\right) \quad ,\alpha = \frac{a}{2D} \\ C_2 &= 4\pi\varepsilon_0\varepsilon_r \cdot a \cdot \left(1+\beta+\frac{\beta^2}{1-\beta^2}+\ldots\right) \quad ,\beta = \frac{a}{2d} \end{aligned} \qquad [4.32]$$

These series are rapidly convergent if $\alpha << 1/2$ and $\beta << 1/2$, which means that as long as the radius of the bubble is much smaller than the distance to the electrodes, C_1 and C_2 can be approximated by

$$\begin{aligned} C_1 &\approx 4\pi\varepsilon_0\varepsilon_r \cdot a \cdot (1+\alpha) = 4\pi\varepsilon_0\varepsilon_r \cdot a \cdot \frac{2D+a}{2D} \\ C_2 &\approx 4\pi\varepsilon_0\varepsilon_r \cdot a \cdot (1+\beta) = 4\pi\varepsilon_0\varepsilon_r \cdot a \cdot \frac{2d+a}{2d} \end{aligned} \qquad [4.33]$$

Then we have

$$\frac{C_1 \cdot C_2}{C_1 + C_2} = 4\pi\varepsilon_0\varepsilon_r \cdot a \cdot \frac{4Dd + 2La + a^2}{8Dd + 2La} \qquad [4.34]$$

which gives the total capacitance C

$$C = C(r,\varepsilon_r) = 4\pi\varepsilon_0\varepsilon_r \cdot r \cdot \frac{r^2 + 2Lr + 4Dd}{2Lr + 8Dd} + \varepsilon_0\varepsilon_r \cdot \frac{S}{L} \qquad [4.35]$$

where L = D+d. Let

$$F(r) = \frac{r^2 + 2Lr + 4Dd}{2Lr + 8Dd} \qquad [4.36]$$

which gives

$$\frac{\partial C}{\partial \varepsilon_r} = 4\pi\varepsilon_0 \cdot r \cdot F(r) + \varepsilon_0 \cdot \frac{S}{L}$$
$$\frac{\partial C}{\partial r} = 4\pi\varepsilon_0\varepsilon_r \cdot (F(r) + r \cdot F'(r)) \qquad [4.37]$$

where

$$F'(r) = \frac{2Lr^2 + 16Ddr + 8LDd}{4L^2r^2 + 32LDdr + 64D^2d^2} \qquad [4.38]$$

I(t) is then

$$I(t) \approx U \cdot \varepsilon_0 \cdot \left[4\pi\varepsilon_r [F(r) + r \cdot F'(r)] \cdot \frac{\Delta r}{\Delta t} + \left[4\pi \cdot r \cdot F(r) + \frac{S}{L} \right] \cdot \frac{\Delta \varepsilon_r}{\Delta t} \right] \qquad [4.39]$$

In fig [4.25], the upper trace shows a current pulse that has a duration of about 15 nanoseconds

$$\Delta t \approx 15 \qquad [\text{ns}]$$

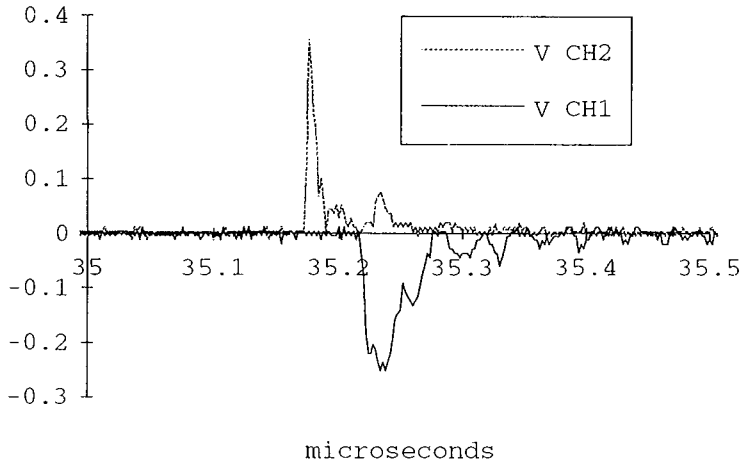

Fig [4.25] Applied voltage +40 kV, laser pulse energy 100 mJ, position 5.
CH2 is current and CH1 is light.

By choosing an appropriate value of the radius (r), it is possible to estimate the magnitudes of Δr and $\Delta\varepsilon_r$ that are needed to produce the observed current pulse. Let us treat Δr and $\Delta\varepsilon_r$ separately. Assume now

that r = 0.5 mm = a, then

$$F(a) = 0.55 \qquad [4.40]$$

$$F'(a) = 100 \qquad [4.41]$$

if the focal spot is placed in the middle of the gap. That is

$$D = d = 2.5 \text{ [mm]} \qquad [4.42]$$

This gives

$$\Delta r = \frac{I(t)\cdot\Delta t}{U\cdot 4\pi\varepsilon_0\varepsilon_r\cdot(F(a)+a\cdot F'(a))}\cdot i_{conv} = 2.7 \quad \text{[mm]} \qquad [4.43]$$

where $i_{conv} = 2.75$ (see section [3.9.1]), U = 40 kV and $\varepsilon_r = 2.2$

$$\Delta\varepsilon_r = \frac{I(t)\cdot\Delta t}{U\cdot\varepsilon_0\cdot\left(4\pi\cdot a\cdot F(a)+\frac{S}{L}\right)}\cdot i_{conv} = 0.344 \qquad [4.44]$$

S has been approximated by the area of a hemisphere of radius 1 cm.

The expansion of the cavity is big! As a matter of fact it is bigger than the gap length. In order to approximate the energy needed for the expansion, we can use equation [4.2]

$$E = 2\pi\rho U^2 R^3 \qquad [4.2]$$

where E is the kinetic energy of the liquid surrounding the bubble, R is the cavity radius, U=dR/dt and ρ is the fluid density. Simplifying by assuming U = constant, the energy needed for the expansion (ΔE) is approximately

$$\Delta E \approx E_2 - E_1 = 2\pi \cdot \rho \cdot U^2 \cdot \left(R_2^3 - R_1^3\right) = 2\pi \cdot \rho \cdot U^2 \cdot \left((R_1 + \Delta r)^3 - R_1^3\right) \qquad [4.45]$$

Substituting for

U = 20*		[m/s]
ρ = 872		[kg/m^3]
R_1 = 0.5		[mm]
Δr = 2.7		[mm]

gives

$$\Delta E = 55 \quad [mJ] \qquad [4.46]$$

This value is too high. Let us compare it with the integrated light emission during this time, see fig [4.25] lower trace. With help of equation [3.19] we get the expression

$$\Delta E_{light} \approx \left[\frac{I \cdot i_{conv}}{I_{tot}} \cdot \Delta t \cdot (\lambda_{c13} - \lambda_{c1})\right] \cdot \frac{hc}{((\lambda_{c13} + \lambda_{c1})/2)} \quad [J] \qquad [4.47]$$

where the term inside the square brackets is the number of photons that produce the light pulse. By assuming that they all have the same wavelength ($\lambda = (\lambda_{c13}+\lambda_{c1})/2$) we get the approximate value

$$\Delta E_{light} \approx 2.14 \cdot 10^{-17} \quad [J] \qquad [4.48]$$

Thus, it seems like the sudden change in capacitance is not mainly due to bubble expansion. Therefore, the main contributor has to be the change in

---

* $\frac{d}{dt}(equation[4.14]) = 0.4 \cdot \left(\frac{E0}{\rho}\right)^{0.2} \cdot \frac{1}{t^{0.6}}$ [m/s]

Substituting for t = 25 μs gives U ≈ 20 [m/s].

the relative dielectric constant.

We have

$$I(t) \approx U \cdot \varepsilon_0 \cdot \left(4\pi \cdot r \cdot F(r) + \frac{S}{L} \right) \cdot \frac{\Delta \varepsilon_r}{\Delta t} \qquad [4.49]$$

This result can be interpreted as the number of charge carriers in the liquid is a main variable, in other words, a correct model has to encounter the number of charges present.

5 DICUSSION

5.1 Conclusions

In this report current and light have been measured. As can be seen in the figures presented , they are well correlated.

The laser triggered breakdown process has been examined by varying four parameters, see chapter 3.

1

- In the experiments with different applied voltages we saw that the measured time lags (T_{lp} and T_{bd}) were exponentially dependent on applied voltage. The polarity of the applied voltage does not seem to influence.

$$T_{bd,lp} \propto |U_{appl}|^k \qquad \text{k = constant}$$

- The large pulse is not observed when the applied voltage is below -35 kV.

- The time lags between large pulse and breakdown (ΔT) seem to have an exponential dependence on applied voltage.

- The pulse density, n_{blp}, seems to be linearly dependent on applied voltage in the positive polarity case. On the other hand when the applied voltage has a negative polarity the density seems to have an exponentially dependence on applied voltage.

2

- Different laser pulse energies caused different time lags. The time to breakdown varied very slowly when the pulse energy exceeded 200 mJ.

- The delay between the large pulse and the breakdown (ΔT) seems to have an exponential dependence on applied energy.

$$\Delta T \propto E^k \qquad \text{k = constant}$$

3

- The location of the focal spot seems to be a main parameter since it caused remarkable differences in the observables. The collected data was used in the analysis in chapter 4.

- The time to the large pulse (T_{LP}) has a maximum when the focal position is in the middle of the gap.

- When the focal spot position is located at the middle of the gap or towards the high voltage electrode, the polarity of the applied voltage does not seem to influence the time to breakdown. However, when the focal spot is located close to the ground electrode, there is a distinct difference in time lags in positive and negative polarity.

- The time lag ΔT between the large pulse and the breakdown is largest when the focal spot is placed near the ground electrode. ΔT reaches a minimum when the focal spot is centered.

(4

- The experiments with different fibre positions showed no variations in the recordings. Later measurements have shown that these results are wrong.**)**

In chapter 4 the laser triggered breakdown process was analysed with help of simple models and the collected data.

- It seems as the breakdown process can be described by five main events:

  1 Trigger mechanism

  2 Expanding cavity

  3 First connecting streamer

  4 Second connecting streamer

  5 Electrical breakdown

- Since the large pulse seem to be immediately preceeded by a propagating streamer, it can be used as a trigger point when studying the streamer phenomenon.

The calm period or the bubble expansion phase has been analysed using a very simple model.

- The discharges that occur inside the cavity, as can be seen as distinct light and current pulses in the recordings, are due to a change of the total capacitance. A rough estimation showed that this change in capacitance is mainly due to a change in the dielectric constant, which shall be interpreted as the number of charge carriers in the liquid is a main parameter.

- The pulse density seems to be a driving force in the prebreakdown process.

5.2 Improvements-new design of the system

The problems with disturbances that I have encountered during my early work, see section [2.2.5], suggest that a great care should be taken with respect to signal transferring and relative position of the equipment. Maybe a shielded room would be appropriate for sensitive equipment such as photomultiplier and oscilloscope, see [5]. As the connecting cables concern, a four time shielded coaxial cable seemed to be good enough.

A stationary fibre arrangement could be made, see fig [5.1].

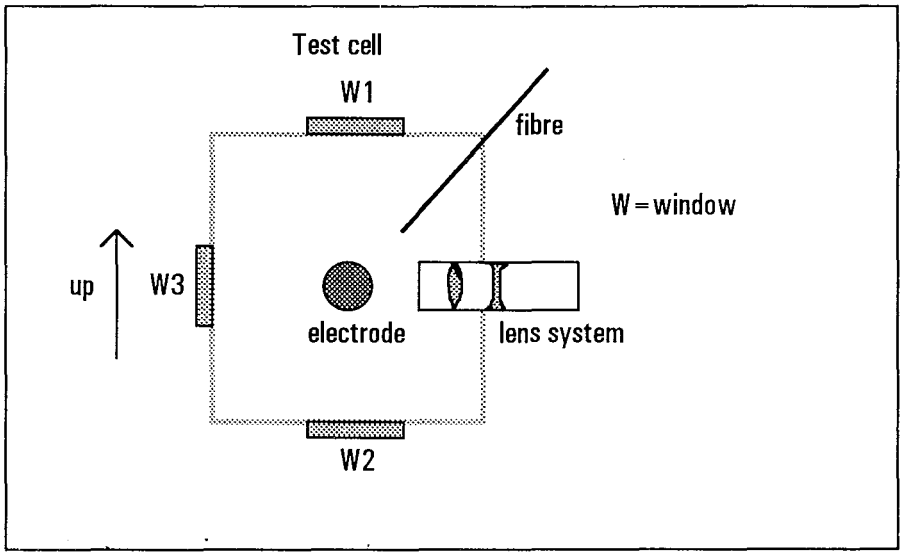

Fig [5.1] Stationary fibre position.

The rest of the windows could then be used for other activities such as photographing etc. In this report the W1 window was used for fibre positioning. A new configuration of the system could then look like fig [5.2].

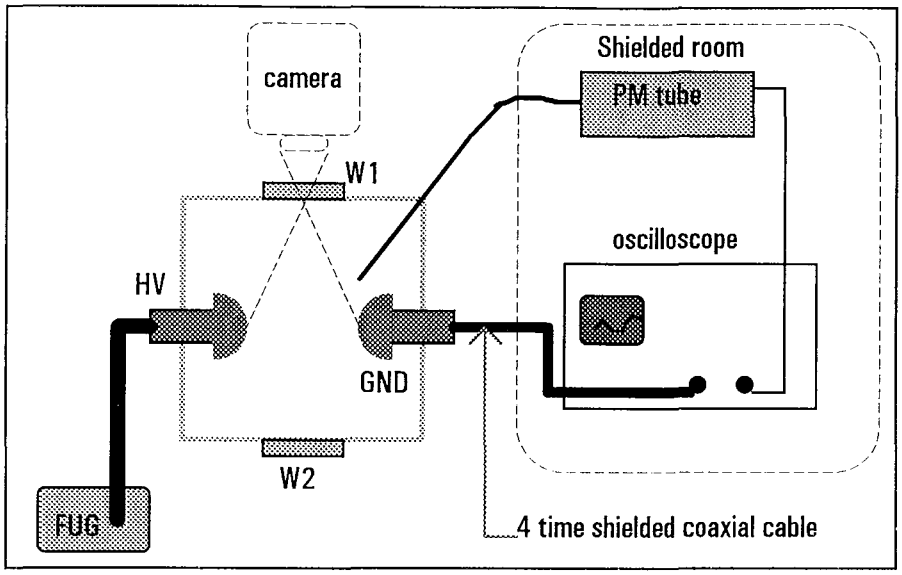

Fig [5.2] A new configuration.

5.2 Further work and investigations

Other liquids than transformer oil (simple ones) should be examined. It would then be possible to analyse more in detail what happens when the laser light hits the liquid.

As mentioned in [21], experiments in longer gaps are needed since the size of the bubble is now in the same range as the gap length.

To be able to further investigate the triggered breakdown process, I think that the photographing technique would be a proper tool. Flash photographs seem to be appropriate while studying bubble dynamics [22].

6 REFERENCES

[1] "Blazing a fiery trail with the hounds"
N. J. Félici
1987 IEEE 9'th International Conference On Conduction and Breakdown in Dielectric Breakdown

[2] "The Dynamics of Pre-Breakdown Cavities in Viscous Silicone Fluids in Negative Point-Plane Gaps"
P. K. Watson, W. G. Chadband
IEEE Trans. Elect. Ins., Vol. 23, No. 4, pp 729-738, 1988

[3] "Prebreakdown Phenomena in Liquid Dielectrics"
A. Béroual, R. Tobazéon
IEEE Trans. Elect. Ins., Vol. EI-21,No. 4, pp 613-627, 1986

[4] "Prebreakdown Phenomena in Hydrocarbon Liquids"
H. Yamashita, H. Amano
IEEE Trans. Elect. Ins., Vol. 23, No. 4, pp 739-750, 1988

[5] "Pre-Breakdown Current and Light Emission Transformer Oil"
H. Yamashita, H. Amano
IEEE Trans. Elect. Ins., Vol. EI-20, No. 2, pp 247-255, 1988

[6] "On the Relation Between Current Pulses and Discharges"
M. I. Qureshi, W. G. Chadband
IEEE Trans. Elect. Ins., Vol. 23, No. 4, pp 715-722, 1988

[7] "Investigations on Transient Currents Associated with Streamer Propagation in Dielectric Liquids"
O. Lesaint, P. Gournay, R. Tobazéon
IEEE Trans. Elect. Ins., Vol. 26, No. 4, pp 699-707, 1991

[8] "Prebreakdown Density Change, Current and Light Emission in Transformer Oil under Non-uniform Field"
H. Yamashita, H. Amano
Journal of Electrostatics, 12 (1982), pp 253-263

[9] "From bubbles to breakdown, or vice-versa"
W. G. Chadband
Proc. of the 11'th Int. Conf. on Conduction and Breakdown in Diel. Liquids (11th ICDL), Baden-Dättwil, pp 184-193, 1993

[10] "Streamer Generation and Propagation in Transformer Oil under ac Divergent Field Conditions"
O. Lesaint, R. Tobazéon
IEEE Trans. Elect. Ins., Vol. 23, No. 6, pp 941-954, 1988

[11] "Generation, growth, and collapse of vapor bubbles in hydrocarbon liquids under a high divergent electric field"
R. Kattan, A. Denat, O. Lesaint
J. Appl. Phys. **66** (9), pp 4062-4066, 1989

[12] "Measurement of Partial Discharges in Hexane under dc Voltage"
E. F. Kelley, M. Nehmadi, R. E. Hebner, M. O. Pace,
A. L. Wintenberg, T. V. Blalock, J. V. Foust
IEEE Trans. Elect. Ins., Vol. 24, No. 6, pp 1109-1119, 1989

[13] "Streamer Propagation in long Point-plane oil gaps"
D. Linhjell, G. Berg, L. Lundgaard
Proc. of the 11'th Int. Conf. on Conduction and Breakdown in Diel. Liquids (11th ICDL), Baden-Dättwil, pp 268-273, 1993

[14] "Behavior of Streamers under Divergent ac Fields in Transformer Oils at Large Gaps"
P. Rain, C. Boisdon, O. Lesaint, R. Tobazéon
IEEE Trans. Elect. Ins., Vol. 26, No. 4, pp 715-725, 1991

[15] "Prebreakdown phenomena in dielectric liquids"
R. Tobazéon
Proc. of the 11'th Int. Conf. on Conduction and Breakdown in Diel. Liquids (11th ICDL), Baden-Dättwil, pp 172-183, 1993

[16] S. S. Hakim, J. B. Higham
Nature **189**, 96, 1961

[17] B. Farazmand
Brit. J. Appl. Phys. **12,** 251, 1961

[18] "Breakdown and Prebreakdown phenomena in liquids"
J. C. Devins, S. J. Rzad, R. J. Schwabe
J. Appl. Phys. **52**(7), pp 4531-4545, 1981

[19] "Electrical breakdown of gases" - book
edited by J. M. Meek, J.D. Craggs
John Wiley & Sons, cop. 1978

[20] "Electrostatic and Hydrodynamic Effects in the Electrical Breakdown of Liquid Dielectrics"
P. K. Watson
IEEE Trans. Elect. Ins., Vol. EI-20, No. 2, pp 395-399, 1985

[21] "Laser-triggering of electric breakdown in liquids"
A. Sunesson, L. Walfridsson
Proc. of the 11'th Int. Conf. on Conduction and Breakdown in Diel. Liquids (11th ICDL), Baden-Dättwil, pp 572-576, 1993

[22] "Bubble Growth Following a Localised Electrical Discharge and its Relationship to the Breakdown of Triggered Spark Gaps in Liquids"
P. K. Watson, W. G. Chadband, W. Y. Mak
IEEE Trans. Elect. Ins., Vol. EI-20, No. 2, pp 275-280, 1985

[23] "High Voltage Engineering Fundamentals" - book
E. Kuffel, W.S. Zaengl
Pergamon Press, 1984

[24] "Field and Wave Electromagnetics" - book
D. K. Cheng
Addison-Wesley, 1989

7 APPENDICES

7.1 Appendix 1

Plasma formation

The Nd:YAG laser used in this work can deliver laser pulses of variable length (t) and energy (Ep), in other words it is possible to choose an appropriate peak power P.

$$P = E_p / t \qquad \text{[A1.1]}$$

If the radius of the focal spot is r, the intensity (I) is given by

$$I = \frac{P}{p \cdot r^2} \qquad \text{[A1.2]}$$

which gives the electric field E

$$E = \sqrt{\frac{2 \cdot I \cdot n}{\varepsilon_r \varepsilon_0 c}} \qquad \text{[A1.3]}$$

where n is the refractive index and c is the speed of light in the medium. One can also express the electric field in terms of the numerical aperture (NA) of the lens.

$$E \propto NA \cdot \sqrt{P} \qquad , NA = \frac{D}{f} \qquad \text{[A1.4]}$$

where D is the beam diameter and f is the focal length. As long as the beam diameter is kept small and the focal length is long, this equation will be valid and we see that the electric field varies linearly with NA [21].This is important as one wishes to avoid self focusing, the self focusing is only a function of optical power and does not depend on NA.

Therefore, it is possible to increase the electric field without affecting the self focusing. A numerical aperture above 0.2 is sufficient to produce a plasma without significant disturbances from self focusing (IR) [21].

7.2 Appendix 2 [Datablad PMT]

7.3 Appendix 3

Light calibration

The notation used here is the same as in section [3.9.2].

λcn [nm]	Φeλn [W/cm^2 nm]	Φe [W/cm^2]	λcn0 [nm]	E=hc/λcn0 [J]	n(λcn0) [# /s cm^2]	A·F(λcn0) [cm^2]	N(λcn0) [# / s]
295	3.4E-08	0.00000312	315	6.306E-19	4.9475E+12	2.571E-09	12718.29
335	1.22E-07	0.0000045	347.5	5.716E-19	7.8721E+12	2.486E-09	19572.08
360	2.38E-07	0.0000144	380	5.227E-19	2.7547E+13	2.239E-08	616858.7
400	4.82E-07	0.00002289	417.5	4.758E-19	4.8109E+13	4.976E-07	23940376
435	8.26E-07	0.00007404	465	4.272E-19	1.7332E+14	1.018E-06	1.76E+08
495	1.642E-06	0.00006615	512.5	3.876E-19	1.7067E+14	1.029E-06	1.76E+08
530	2.138E-06	0.0000954	550	3.612E-19	2 6414E+14	1.018E-06	2.69E+08
570	2.632E-06	0.000114	590	3.367E-19	3.386E+14	1.018E-06	3.45E+08
610	3.068E-06	0.00011456	627.5	3.166E-19	3.6187E+14	1.271E-06	4.6E+08
645	3.478E-06	0.00007171	655	3.033E-19	2.3645E+14	1.541E-06	3.64E+08
665	3.693E-06	0.00046868	722.5	2.749E-19	1.7047E+15	5.091E-06	8.68E+09
780	4.458E-06	0.00032673	815	2.437E-19	1.3405E+15	9.951E-06	1.33E+10
850	4.877E-06						

λcn [nm]	Yn [V]	Un [V]	In=Un/R [A]	in=In/N [As / #]	Δλ [#]	ΔItot [As]
295	0.01264	2E-05	4E-07	3.145E-11	40	1.258E-09
335	0.01262	2E-05	4E-07	2.044E-11	25	5.109E-10
360	0.0126	6E-05	1.2E-06	1.945E-12	40	7.781E-11
400	0.01254	7E-05	1.4E-06	5.848E-14	35	2.047E-12
435	0.01247	0.00031	6.2E-06	3.514E-14	60	2.108E-12
495	0.01216	0.00029	5.8E-06	3.301E-14	35	1.156E-12
530	0.01187	0.0004	8E-06	2.975E-14	40	1.19E-12
570	0.01147	0.0006	0.000012	3.481E-14	40	1.392E-12
610	0.01087	0.00085	0.000017	3.695E-14	35	1.293E-12
645	0.01002	0.0013	0.000026	7.134E-14	20	1.427E-12
665	0.00872	0.00487	0.0000974	1.122E-14	115	1.291E-12
780	0.00385	0.001	0.00002	1.499E-15	70	1.05E-13
850	0.00285				Itot	Σ 1.859E-09

Φ_e has been calculated using the formula

$$\Phi e = \frac{1}{2} \cdot (\lambda_{c(n+1)} - \lambda_{cn}) \cdot (\Phi_{e\lambda n} + \Phi_{e\lambda(n+1)}) \quad \left[\frac{W}{cm^2}\right] \qquad [A3.1]$$

and λ_{cn0} is given by

$$\lambda_{cn0} = \frac{\lambda_{cn} + \lambda_{c(n+1)}}{2} \quad [nm] \qquad [A3.2]$$

7.4 Appendix 4

Sphere outside a plane

By repeated application of the method of images it is possible to solve the problem with a charged sphere outside a grounded plane. The method results in two groups of image point charges, that together make the sphere and the plane equipotential. Since the charges cancel out in pairs it is easy to calculate the potential of the sphere.

$$V_0 = \frac{Q_0}{4\pi\varepsilon \cdot a} \qquad [A4.1]$$

The charge Q on the sphere is

$$Q = Q_0 + Q_1 + Q_2 + \ldots = Q_0 \cdot \left(1 + \alpha + \frac{\alpha^2}{1-\alpha^2} + \ldots\right) \qquad [A4.2]$$

where α=a/2c. Hence, the capacitance between the sphere and the conducting plane is [24].

$$C = \frac{Q}{V_0} = 4\pi\varepsilon \cdot \left(1 + \alpha + \frac{\alpha^2}{1-\alpha^2} + \ldots\right) \qquad [A4.3]$$

The series converges rapidly if $\alpha < 1/2$

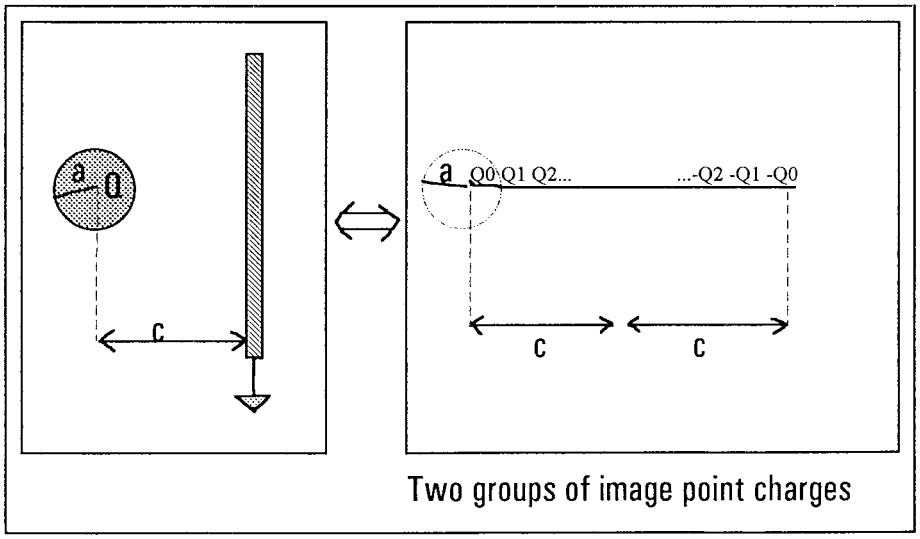

Fig [A4.1] Physical arrangement and its equivalence.

One can observe that the expression of the capacitance is not dependent of the charge on the sphere. It only depends on geometric parameters. Therefore is the capacitance of a charged sphere outside a charged plane the same.